Noname manuscript No.
(will be inserted by the editor)

Grégory Schehr · Satya N. Majumdar · Alain Comtet · Peter J. Forrester

Reunion probability of N vicious walkers: typical and large fluctuations for large N

October 9, 2012

Abstract We consider three different models of N non-intersecting Brownian motions on a line segment $[0, L]$ with absorbing (model A), periodic (model B) and reflecting (model C) boundary conditions. In these three cases we study a properly normalized reunion probability, which, in model A, can also be interpreted as the maximal height of N non-intersecting Brownian excursions (called "watermelons" with a wall) on the unit time interval. We provide a detailed derivation of the exact formula for these reunion probabilities for finite N using a Fermionic path integral technique. We then analyse the asymptotic behavior of this reunion probability for large N using two complementary techniques: (i) a saddle point analysis of the underlying Coulomb gas and (ii) orthogonal polynomial method. These two methods are complementary in the sense that they work in two different regimes, respectively for $L \ll O(\sqrt{N})$ and $L \geq O(\sqrt{N})$. A striking feature of the large N limit of the reunion probability in the three models is that it exhibits a third-order phase transition when the system size L crosses a critical value $L = L_c(N) \sim \sqrt{N}$. This transition is akin to the Douglas-Kazakov transition in two-dimensional continuum Yang-Mills theory. While the central part of the reunion probability, for $L \sim L_c(N)$, is described in terms of the Tracy-Widom distributions (associated to GOE and GUE depending on the model), the emphasis of the present study is on the large deviations of these reunion probabilities, both in the right $[L \gg L_c(N)]$ and the left $[L \ll L_c(N)]$ tails. In particular, for model B, we find that the matching between the different regimes corresponding to typical $L \sim L_c(N)$ and atypical fluctuations in the right tail $L \gg L_c(N)$ is rather unconventional, compared to the usual behavior

G. Schehr
Laboratoire de Physique Théorique et Modèles Statistiques, Université Paris-Sud, Bât. 100, 91405 Orsay Cedex, France

S. N. Majumdar
Laboratoire de Physique Théorique et Modèles Statistiques, Université Paris-Sud, Bât. 100, 91405 Orsay Cedex, France

A. Comtet
Laboratoire de Physique Théorique et Modèles Statistiques, Université Paris-Sud, Bât. 100, 91405 Orsay Cedex, France
Université Pierre et Marie Curie-Paris 6, 75005, Paris, France

P. J. Forrester
Department of Mathematics and Statistics, The University of Melbourne, Victoria 3010, Australia

found for the distribution of the largest eigenvalue of GUE random matrices. This paper is an extended version of [G. Schehr, S. N. Majumdar, A. Comtet, J. Randon-Furling, Phys. Rev. Lett. **101**, 150601 (2008)] and [P. J. Forrester, S. N. Majumdar, G. Schehr, Nucl. Phys. B **844**, 500-526 (2011)].

1 Introduction

Non-intersecting random walkers, first introduced by de Gennes [1], followed by Fisher [2] (who called them "vicious walkers"), have been studied extensively in statistical physics as they appear in a variety of physical contexts ranging from wetting and melting all the way to polymers and vortex lines in superconductors. Lattice versions of such walkers also have beautiful combinatorial properties [3]. Non-intersecting Brownian motions, defined in continuous space and time, have also recently appeared in a number of contexts. In particular their connection to the random matrix theory has been noted in a variety of situations [4–18]. Rather recently, we have unveiled an unexpected connection between vicious walkers and two-dimensional continuum Yang-Mills theory on the sphere with a given gauge group G [19], which depends on the boundary conditions in the vicious walkers problem (a different type of connection between the Yang-Mills theory and vicious walkers problems had also been noticed in Ref. [20]).

Specifically, we consider a set of N non-intersecting Brownian motions on a finite segment $[0, L]$ of the real line with different boundary conditions. Assuming that all the walkers start from the vicinity of the origin, we then define the reunion probability as the probability that the walkers reunite at the origin after a fixed interval of time which can be set to unity without any loss of generality. Within the time interval $[0, 1]$, the walkers stay non-intersecting. Next we 'normalize' this reunion probability in a precise way to be defined shortly. In one case, namely when both boundaries at 0 and L are absorbing, one can relate this 'normalized' reunion probability to the probability distribution of the maximal height of N non-intersecting Brownian excursions. In Ref. [19] it was shown that this normalized reunion probability in the Brownian motion models maps onto the exactly solvable partition function (up to a multiplicative factor) of two-dimensional Yang-Mills theory on a sphere. The boundary conditions at the edges 0 and L select the gauge group G of the associated Yang-Mills theory. We consider three different boundary conditions: absorbing (model A), periodic (model B), and reflecting (model C) which correspond respectively to the following gauge groups in the Yang-Mills theory: (A) absorbing $\to$ Sp($2N$), (B) periodic $\to$ U(N) and (C) reflecting $\to$ SO($2N$). As a consequence of this connection, in each of these Brownian motion models, as one varies the system size L, a third order phase transition occurs at a critical value $L = L_c(N) = \mathcal{O}(\sqrt{N})$ in the large N limit. It was shown in Ref. [21] that a similar third order phase transition also occurs for the probability distribution function of the largest eigenvalue of random matrices belonging to the standard Gaussian ensembles. Furthermore, third order phase transitions in the large deviation function of appropriate variables have also been found recently in a variety of other problems, such as in the distribution of conductance through a mesoscopic cavity such as a quantum dot [22–24] and in the distribution of the entanglement entropy in a bipartite random pure state [25, 26].

Close to the critical point, these reunion probabilities in the Brownian motion models, properly shifted and scaled, can be related to the Tracy-Widom (TW) distributions. Let us briefly remind the readers about the Tracy-Widom distributions. Tracy-Widom distribution describes the limiting form of the distribution of the scaled largest eigenvalue in the three classical Gaussian random matrix ensembles [27]. These limiting distributions are usually denoted by $\mathcal{F}_1(t)$ for the Gaussian orthogonal ensemble (GOE), by $\mathcal{F}_2(t)$ for the Gaussian unitary ensemble (GUE) and by $\mathcal{F}_4(t)$ for the Gaussian symplectic ensemble (GSE). For example, in the GUE case where one considers the set of $N \times N$ complex Hermitian matrices X with measure proportional to $e^{-\mathrm{Tr}X^2}$ and denote $\lambda_{\max}$ the largest eigenvalue, the typical fluctuations around its mean value

$\langle \lambda_{\max} \rangle \simeq \sqrt{2N}$ have a limiting distribution [27]

$$\lim_{N\to\infty} \Pr\left(\sqrt{2} N^{\frac{1}{6}} (\lambda_{\max} - \sqrt{2N}) < t \right) = \exp\left(- \int_t^\infty (s-t) q^2(s) ds \right) := \mathcal{F}_2(t), \tag{1}$$

known as the $\beta = 2$ Tracy-Widom distribution. In Eq. (1), $q(s)$ satisfies Painlevé II (PII) differential equation

$$q''(s) = s q(s) + 2 q^3(s) \ , \tag{2}$$

with the asymptotic behavior

$$q(s) \sim \mathrm{Ai}(s) \, \text{as} \ s \to \infty \ , \tag{3}$$

where $\mathrm{Ai}(s)$ is the Airy function. One can indeed show that this asymptotic behavior (3) determines a unique solution of PII (2), known as the Hastings-McLeod solution. Similarly, the distribution $\mathcal{F}_1$ concerns real symmetric matrices. Explicitly, with the GOE specified as the set of $N \times N$ real symmetric matrices X with measure proportional to $e^{-\mathrm{Tr} X^2/2}$, and $\lambda_{\max}$ denoting the largest eigenvalue, one has [28]

$$\begin{aligned} \lim_{N\to\infty} \Pr\left(\sqrt{2} N^{\frac{1}{6}} (\lambda_{\max} - \sqrt{2N}) < t \right) \ &= \ \exp\left(- \frac{1}{2} \int_t^\infty \left((s-t) \, q^2(s) + q(s) \right) \, ds \right) \\ &:= \mathcal{F}_1(t) \ , \end{aligned} \tag{4}$$

known as the $\beta = 1$ Tracy-Widom distribution. Because of their relevance in many fundamental problems in mathematics and physics, these TW distributions have been widely studied in the literature. In particular, their asymptotic behaviors are given, to leading order by

$$\begin{cases} \mathcal{F}_\beta(t) \sim \exp\left(-\frac{\beta}{24} |t|^3 \right) \ , \ t \to -\infty \ , \\ \\ 1 - \mathcal{F}_\beta(t) \sim \exp\left(-\frac{2\beta}{3} t^{3/2} \right) \ , \ t \to \infty \end{cases} \tag{5}$$

where $\beta = 1$ and $\beta = 2$ correspond respectively to the GOE and the GUE case.

Our study of constrained vicious walkers problems started in Ref. [12] where we derived, using a Fermionic path integral method, an exact expression for the ratio of reunion probability, for model A and for any finite number N of walkers. This calculation, in this specific case, was motivated by the interpretation of this ratio in terms of an extreme value quantity, namely the maximal height of N non-intersecting Brownian excursions, which is recalled below in section 2 (see also Fig. 1). We showed later in Ref. [19] that this ratio, and its extension to other boundary conditions in model B and C, is actually equal, up to a multiplicative prefactor, to the partition function of Yang-Mills theory on the sphere with a given gauge group G, which depends on the boundary conditions in the vicious walkers problem. Following the pioneering works of Refs. [29,30] where the large N analysis of Yang-Mills theory on the sphere with the gauge group $G = \mathrm{U}(N)$, and extended to other classical Lie groups, including $G = \mathrm{Sp}(2N)$ or $G = \mathrm{SO}(2N)$, in Ref. [31], we could also perform in Ref. [19] the large N analysis of these reunion probabilities. However, most of these results were announced in Refs. [12,19] without any detail. The purpose of the present paper is to give a self-contained derivation of these results, both for finite and large N. For large N we characterize not only the distribution of typical fluctuations, which can be expressed in terms of $\mathcal{F}_1$ and $\mathcal{F}_2$ but also provide a detailed analysis of the large deviations of these reunion probabilities, characterizing atypical fluctuations. A special emphasis is put on the matching between different regimes (typical and atypical) of the reunion probability as a function of L. In particular, for the case of periodic boundary conditions, we find that the matching found in this vicious walker problem is quite different from the corresponding matching observed in the

distribution of the largest eigenvalue of Gaussian random matrices in the unitary ensemble [13, 32–37].

The paper is organized as follows. In section 2 we describe the three models A, B and C and summarize the main results for the ratio of reunion probabilities in the large N limit. In section 3 we give the details of the path integral method which allows us to obtain an exact expression of these ratios in each of the three models for any finite N and L. In section 4, we compute the large N limit of this ratio for model A and analyze in detail the typical fluctuations (namely the central part of the distribution) as well as the large deviations: both for the left and for the right tails. The corresponding large N analysis for model B and C are performed in section 5 and section 6, respectively, before we conclude in section 7. Some details have been relegated to Appendix A.

2 Models and main results

We consider three different models of N non-intersecting Brownian walkers on a one-dimensional line segment $[0, L]$ and label their positions at time τ by $x_1(\tau) < \ldots < x_N(\tau)$. These three models, denoted by model A, B and C, differ by the boundary conditions which are imposed at $x = 0$ and $x = L$:

• in model A, we consider absorbing boundary conditions both at $x = 0$ and $x = L$,

• in model B, we study periodic boundary conditions, which amounts to consider N non-intersecting Brownian motions on a circle of radius $L/2\pi$,

• and in model C we consider reflecting boundary conditions both at $x = 0$ and $x = L$.

	Model A	Model B	Model C
Boundary conditions at $x = 0$ and $x = L$	absorbing	periodic	reflecting
Corresponding affine Weyl chamber	$\tilde{C}_N$	$\tilde{A}_{N-1}$	$\tilde{B}_N$
Gauge group of the associated YM_2 theory	Sp($2N$)	U(N)	SO($2N$)

Table 1 Summary of our results for the three different models A, B and C.

Model A: In the first model the domain is the line segment $[0, L]$ with *absorbing boundary conditions at both boundaries* 0 *and* L. This corresponds to N-dimensional Brownian motion in an affine Weyl chamber of type $\tilde{C}_N$ [39,40]. The N non-intersecting Brownian motions start initially at the positions, say, $\{\epsilon_1, \epsilon_2, \ldots, \epsilon_N\}$ in the vicinity of the origin where eventually we will take the limit $\epsilon_i \to 0$ for all i, as shown later. We define the reunion probability $R_L^A(1)$, where the superscript 'A' refers to model A, as the probability that the walkers return to their initial positions after a fixed time $\tau = 1$ (staying non-intersecting over the time interval $\tau \in [0, 1]$). We define the normalized reunion probability

$$\tilde{F}_N(L) = \frac{R_L^A(1)}{R_\infty^A(1)} \,, \tag{6}$$

such that $\lim_{L\to\infty} \tilde{F}_N(L) = 1$. This ratio becomes independent of the starting positions ϵ_i's in the limit when $\epsilon_i \to 0$ for all i, as shown later. Hence, $\tilde{F}_N(L)$ depends only on N and L.

This ratio $\tilde{F}_N(L)$ in Model A has also a different probabilistic interpretation. Consider the same model but now on the semi-infinite line $[0,\infty)$ with still absorbing boundary condition at 0. The walkers, as usual, start in the vicinity of the origin and are conditioned to return to the origin exactly at $\tau = 1$ (see Fig. 1). If one plots the space-time trajectories of the walkers, a typical configuration looks like half of a watermelon (see Fig. 1), or a watermelon in presence of an absorbing wall. Such configurations of Brownian motions are known as non-intersecting Brownian excursions [10] and their statistical properties have been studied quite extensively in the recent past. A particular observable that has generated some recent interests is the so-called 'height' of the watermelon [12,38,41–46] defined as follows (see also Ref. [47] for a related quantity in the context of Dyson's Brownian motion). Let H_N denote the maximal displacement of the rightmost walker x_N in this time interval $\tau \in [0,1]$, i.e., the maximal height of the topmost path in half-watermelon configuration (see Fig. 1), i.e., $H_N = \max_\tau\{x_N(\tau), 0 < \tau < 1\}$. This global maximal height H_N is a random variable which fluctuates from one configuration of half-watermelon to another. What is the probability distribution of H_N? For $N = 1$ the distribution of H_N is easy to compute and already for $N = 2$ it is somewhat complicated [42]. In Ref. [12] an exact formula for the distribution of H_N, valid for all N, was derived using Fermionic path integral method, which we remind below for consistency (see also [42–44] for a derivation using different methods). The distribution of H_N, in the large N limit, is quite interesting as it gives, in the proper scaling limit, the distribution of the maximum (on the real line) of the Airy_2 process minus a parabola [6,48,49]. This latter process describes the universality class of the Kardar-Parisi-Zhang (KPZ) equation in the so-called "droplet" geometry. It was known rather indirectly from the work of Ref. [6] on the Airy_2 process that the limiting distribution of H_N should then be given by $\mathcal{F}_1$. This was one of the main result of Ref. [19] to show this result by a direct computation of the limiting distribution of H_N. This result, for the vicious walkers problem, was then recently proved rigorously in [46] using Riemann-Hilbert techniques. In Ref. [50] a direct and rigorous proof was established that the distribution of the maximum of Airy_2 minus a parabola is indeed given by $\mathcal{F}_1$. We refer the reader to Refs. [51–53] for more recent results on the extreme statistics of the Airy_2 process minus a parabola. We also mention that the limiting distribution of H_N was measured in recent experiments on liquid crystals, and a very good agreement with $\mathcal{F}_1$ was indeed found [54].

To relate the distribution of H_N in the semi-infinite system defined above to the ratio of reunion probabilities in the finite segment $[0, L]$ defined in (6), it is useful to consider the cumulative probability $\Pr(H_N \le L)$ in the semi-infinite geometry, where L now is just a variable. To compute this cumulative probability, we need to calculate the fraction of half-watermelon configurations (out of all possible half-watermelon configurations) that never cross the level L, i.e., whose heights stay below L over the time interval $\tau \in [0,1]$ (see Fig. 1). This fraction can be computed by putting an absorbing boundary at L (thus killing all configurations that touch/cross the level L). It is then clear that $\Pr(H_N \le L)$ is nothing but the normalized reunion probability $\tilde{F}_N(L)$ defined in (6). As mentioned above, this cumulative probability distribution of the maximal height was computed exactly in Ref. [12]

$$\begin{aligned}\tilde{F}_N(L) &:= \Pr(H_N \le L) \\ &= \frac{A_N}{L^{2N^2+N}} \sum_{n_1=-\infty}^{\infty} \cdots \sum_{n_N=-\infty}^{\infty} \Delta^2(n_1^2,\ldots,n_N^2)\Big(\prod_{j=1}^{N} n_j^2\Big) e^{-\frac{\pi^2}{2L^2}\sum_{j=1}^{N} n_j^2}\,, \end{aligned} \tag{7}$$

where

$$\Delta_N(y_1,\ldots,y_N) = \prod_{1\le i<j\le N} (y_i - y_j) \tag{8}$$

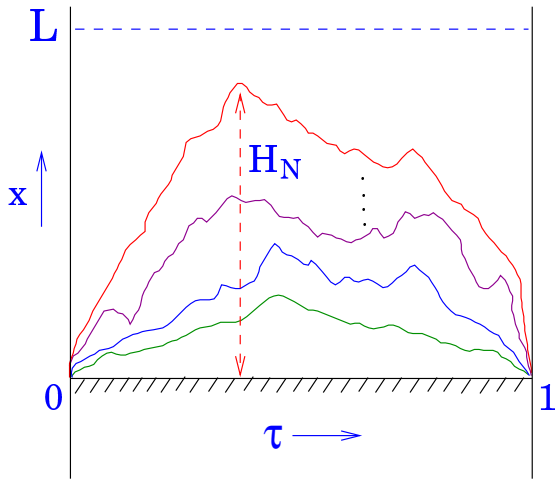

Fig. 1 Trajectories of N non-intersecting Brownian motions $x_1(\tau) < x_2(\tau) < \ldots < x_N(\tau)$, all start at the origin and return to the origin at $\tau = 1$, staying positive in between. $\tilde{F}_N(L)$ denotes the probability that the maximal height $H_N = \max_\tau\{x_N(\tau), 0 \leq \tau \leq 1\}$ stays below the level L over the time interval $0 \leq \tau \leq 1$.

is the Vandermonde determinant and where the amplitude is given by

$$A_N = \frac{\pi^{2N^2+N}}{2^{N^2+N/2}\prod_{j=0}^{N-1}\Gamma(2+j)\Gamma(3/2+j)} \,. \tag{9}$$

This quantity $\tilde{F}_N(L)$ was also computed in Refs. [43,44] using different methods. In Ref. [43] the authors studied the maximal height of N non-intersecting Brownian excursions and used the Karlin-McGregor formula [55]. In Ref. [44] the author computed the cumulative distribution of the maximal height of N-non intersecting discrete lattice paths (of n discrete steps) in presence of a wall, using the Lindström-Gessel-Viennot formula [56,57], and then he considered the asymptotic limit of a large number of steps n. The formulas obtained using these two similar methods are actually different from the one given in Eq. (7) obtained by using a fermionic path integral and it is a non-trivial task to check, as expected, that they are indeed equivalent to (7) [43]. A derivation of the formula given above in Eqs. (7, 9), which turns out to be the most convenient expression of $\tilde{F}_N(L)$ in view of a large N asymptotic analysis, is given in section 3. Remarkably, if one denotes by

$$\mathcal{Z}(A, G) \tag{10}$$

the partition function of the two-dimensional (continuum) Yang-Mills theory on the sphere (denoted as YM_2) with gauge group G and area A it was shown in Ref. [19] that $\tilde{F}_N(L)$ is related to YM_2 with the gauge group $G = \mathrm{Sp}(2N)$ via the relation

$$\tilde{F}_N(L) \propto \mathcal{Z}\left(A = \frac{2\pi^2}{L^2}\, N, \mathrm{Sp}(2N)\right) \,. \tag{11}$$

In Ref. [29,31], it was shown that for large N, $\mathcal{Z}(A, \mathrm{Sp}(2N))$ exhibits a third order phase transition at the critical value $A = \pi^2$ separating a weak coupling regime for $A < \pi^2$ and a strong coupling regime for $A > \pi^2$. This is the so called Douglas-Kazakov phase transition [29], which is the counterpart in continuum space-time, of the Gross-Witten-Wadia transition [58,59] found in two-dimensional lattice quantum chromo-dynamics (QCD), which is also of third order. Using the correspondence $L^2 = 2\pi^2 N/A$, we then find that $\tilde{F}_N(L)$, considered as a function of L with N large but fixed, also exhibits a third order phase transition at the critical value $L_c(N) = \sqrt{2N}$. Furthermore, the weak coupling regime ($A < \pi^2$) corresponds to $L > \sqrt{2N}$ and thus describes the right tail of $\tilde{F}_N(L)$, while the strong coupling regime corresponds to $L < \sqrt{2N}$ and describes instead the left tail of $\tilde{F}_N(L)$ (see Fig. 2). The critical regime around $A = \pi^2$ is the so called "double scaling" limit in the matrix model and has width of order $N^{-2/3}$. It corresponds to the region of width $\mathcal{O}(N^{-1/6})$ around $L = \sqrt{2N}$ where $\tilde{F}_N(L)$, correctly shifted and scaled, is described by the Tracy-Widom distribution $\mathcal{F}_1(t)$ in Eq. (4).

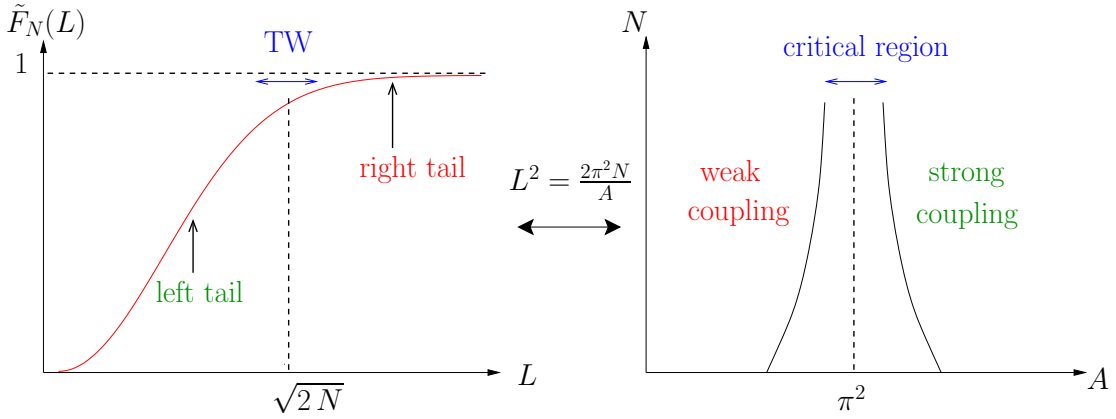

Fig. 2 Left: Schematic sketch of $\tilde{F}_N(L)$ as defined in Eq. (7) for N vicious walkers on the line segment $[0, L]$ with absorbing boundary conditions at both ends, as a function of L, for fixed but large N. **Right:** Sketch of the phase diagram in the plane (A, N) of two-dimensional Yang-Mills theory on a sphere with the gauge group $\mathrm{Sp}(2N)$ as obtained in Ref. [29,31]. The weak (strong) coupling phase in the right panel corresponds to the right (left) tail of $\tilde{F}_N(L)$ in the left panel. The critical region around $A = \pi^2$ in the right panel corresponds to the Tracy-Widom (TW) regime in the left panel around the critical point $L_c(N) = \sqrt{2N}$.

Although the occurrence of the Painlevé transcendent $q(s)$ (2) in this double scaling limit was known since the work of Periwal and Shevitz [60], its probabilistic interpretation in relation to the Tracy-Widom distribution was one of the main achievements of Ref. [19]. In this paper, we provide a detailed analysis of the three regimes: the left tail, the central part and the right tail of $\tilde{F}_N(L)$. Our results can be summarized as follows

$$\begin{cases} \tilde{F}_N(L) & \sim \exp\left[-N^2 \phi_-^A\left(L/\sqrt{2N}\right)\right] \,, \; L < \sqrt{2N} \;\&\; |L - \sqrt{2N}| \sim \mathcal{O}(\sqrt{N}) \\ \tilde{F}_N(L) & \sim \mathcal{F}_1\left[2^{11/6} N^{1/6} (L - \sqrt{2N})\right] \,, \; L \sim \sqrt{2N} \;\&\; |L - \sqrt{2N}| \sim \mathcal{O}(N^{-1/6}) \\ 1 - \tilde{F}_N(L) & \sim \exp\left[-N \phi_+^A\left(L/\sqrt{2N}\right)\right] \,, \; L > \sqrt{2N} \;\&\; |L - \sqrt{2N}| \sim \mathcal{O}(\sqrt{N}) \,, \end{cases} \tag{12}$$

where $\mathcal{F}_1$ is the TW distribution for GOE, whose explicit expression is given in (4) and its asymptotic behaviors are given in Eq. (5). The rate functions $\phi_\pm^A(x)$ can be computed exactly

(see later): of particular interest are their asymptotic behaviors when $L \to \sqrt{2N}$ from below (left tail) and from above (right tail), which are given by

$$\phi_-^A(x) \sim \frac{16}{3}(1-x)^3 \ , \ x \to 1^- \ , \tag{13}$$
$$\phi_+^A(x) \sim \frac{2^{9/2}}{3}(x-1)^{3/2} \ , \ x \to 1^+ \ .$$

The different behavior of $\tilde{F}_N(L)$ in Eq. (12) for $L < \sqrt{2N}$ and $L > \sqrt{2N}$ leads, in the limit $N \to \infty$ to a phase transition at the critical point $L = \sqrt{2N}$ in the following sense. Indeed if one scales L by $\sqrt{2N}$, keeping the ratio $x = L/\sqrt{2N}$ fixed, and take the limit $N \to \infty$ one obtains

$$\lim_{N\to\infty} -\frac{1}{N^2} \ln \tilde{F}_N \left(x = \frac{L}{\sqrt{2N}} \right) = \begin{cases} \phi_-^A(x) \ , \ x < 1 \\ 0 \ , \ x > 1 \ . \end{cases} \tag{14}$$

If one interprets $\tilde{F}_N(L)$ in Eq. (7) as the partition function of a discrete Coulomb gas, its logarithm can be interpreted as its free energy. Since $\phi_-^A(x) \sim (1-x)^3$ when x approaches 1 from below, then the third derivative of the free energy at the critical point $x = 1$ is discontinuous, which can then be interpreted as a third order phase transition.

On the other hand, comparing the asymptotic behavior of $\mathcal{F}_1$ in Eq. (5) with the ones of the rate functions (13) we can check that the expansion of the large deviation functions around the transition point coincides with the tail behaviors of the central region Tracy-Widom scaling function. This property holds here both for the left and the right tails. For instance, consider first the left tail in Eq. (12), i.e., when $L \ll \sqrt{2N}$. When $L \to \sqrt{2N}$ from below, we can substitute the asymptotic behavior of the rate function $\phi_-^A(x)$ from Eq. (13) in the first line of Eq. (12). This gives

$$\tilde{F}_N(L) \sim \exp\left(-\frac{2^{5/2}}{3} N^{1/2} (\sqrt{2N} - L)^3 \right) \ , \ 1 \ll \sqrt{2N} - L \ll \sqrt{2N} \ , \tag{15}$$

On the other hand, consider now the second line of Eq. (12) that describes the central typical fluctuations. When the deviation from the mean is large, i.e., $\sqrt{2N} - L \sim O(\sqrt{N})$ (compared to the typical scale $\sim O(N^{-1/6})$), we can substitute in the second line of Eq. (12) the left tail asymptotic behavior of the Tracy-Widom function $\mathcal{F}_1(t)$ as described in the first line of Eq. (5) (with $\beta = 1$). This gives,

$$\tilde{F}_N(L) \sim \exp\left[-\frac{1}{24} \left(2^{11/6} N^{1/6} (\sqrt{2N} - L) \right)^3 \right] \tag{16}$$

which, after a trivial rearrangement, is identical to the expression in Eq. (15). Thus the left tail of the central region matches smoothly with the left large deviation function. Similarly, on the right side, using the behavior of $\phi_+^A(x)$ in Eq. (13), one finds from Eq. (12), that

$$1 - \tilde{F}_N(L) \sim \exp\left(-\frac{2^{15/4}}{3} N^{1/4} (L - \sqrt{2N})^{3/2} \right) \ , \ 1 \ll L - \sqrt{2N} \ll \sqrt{2N} \ , \tag{17}$$

which matches perfectly with the right tail of the central part described by $\mathcal{F}_1(t)$ (5, 12). Hence in this case of model A, the matching between the different regimes is similar to the one found in previous studies of large deviation formulas associated with the largest eigenvalue of random matrices [13,32–36].

Model B: In the second model we consider periodic boundary conditions on the line segment $[0, L]$. Alternatively, one can think of the domain as a circle of circumference L (of radius $L/2\pi$).

This corresponds to N-dimensional Brownian motion in an affine Weyl chamber of type $\tilde{A}_{n-1}$ [39, 40]. All walkers start initially in the vicinity of a point on the circle which we call the origin. We can label the positions of the walkers by their angles $\{\theta_1, \theta_2, \dots, \theta_N\}$ (see section 3 for details). Let the initial angles be denoted by $\{\epsilon_1, \epsilon_2, \dots, \epsilon_N\}$ where ϵ_i's are small. Eventually we will take the limit $\epsilon_i \to 0$. We denote by $R_L^B(1)$ the reunion probability after time $\tau = 1$ (note that the walkers, in a bunch, may wind the circle multiple times), i.e, the probability that the walkers return to their initial positions after time $\tau = 1$ (staying non-intersecting over the time interval $\tau \in [0, 1]$). Evidently $R_L^B(1)$ depends on N and also on the starting angles $\{\epsilon_1, \epsilon_2, \dots, \epsilon_N\}$. To avoid this additional dependence on the ϵ_i's, let us introduce the normalized reunion probability defined as the ratio

$$\tilde{G}_N(L) = \frac{R_L^B(1)}{R_\infty^B(1)} \,, \tag{18}$$

where we assume that we have taken the $\epsilon_i \to 0$ limit. One can actually check that the ϵ_i's dependence actually cancels out between the numerator and the denominator: this is the main motivation for studying this ratio of reunion probabilities (18) in this case. Although in the case of model A it is rather natural to expect that this limit $\epsilon_i \to 0$ is well defined, given the interpretation of $\tilde{F}_N(L)$ as the cumulative distribution of the maximal height of non-intersecting excursions, this is not so obvious for $\tilde{G}_N(L)$ where such an interpretation does not exist. Nevertheless one can show that this property also holds in this case, yielding (see Ref. [19] and also section 3)

$$\tilde{G}_N(L) = \frac{B_N}{L^{N^2}} \sum_{n_1=-\infty}^{\infty} \dots \sum_{n_N=-\infty}^{\infty} \Delta_N^2(n_1, \dots, n_N) e^{-\frac{2\pi^2}{L^2}\sum_{j=1}^N n_j^2} \,, \tag{19}$$

where $\Delta_N(n_1, \dots, n_N)$ is the Vandermonde determinant (8) and the prefactor

$$B_N = \frac{1}{(2\pi)^{N/2-N^2} \prod_{j=0}^{N-1} \Gamma(j+2)} \tag{20}$$

ensures that $\tilde{G}_N(L \to \infty) = 1$. In Ref. [19] it was shown that this normalized reunion probability $\tilde{G}_N(L)$ is, up to a prefactor, exactly identical to the partition function of the 2-d Yang-Mills theory on a sphere with gauge group $\mathrm{U}(N)$:

$$\tilde{G}_N(L) \propto \mathcal{Z}\left(A = \frac{4\pi^2 N}{L^2}, \mathrm{U}(N)\right) \,. \tag{21}$$

This partition function $\mathcal{Z}(A, \mathrm{U}(N))$ exhibits the Douglas-Kazakov third order phase transition for $A = \pi^2$ which means that in that case the transition between the right tail and the left tail behavior of $\tilde{G}_N(L)$ occurs for $L = L_c(N) = \sqrt{4N}$. In this paper, we provide a detailed analysis of the various regimes, right tail, central part and left tail of $\tilde{G}_N(L)$. Our results can be summarized as follows

$$\begin{cases} \tilde{G}_N(L) & \sim \exp\left[-N^2 \phi_-^B\left(L/\sqrt{4N}\right)\right] \,,\ L < \sqrt{4N} \ \&\ |L - \sqrt{4N}| \sim \mathcal{O}(\sqrt{N}) \\ \tilde{G}_N(L) & \sim \mathcal{F}_2\left[2^{2/3} N^{1/6} (L - \sqrt{4N})\right] \,,\ L \sim \sqrt{4N} \ \&\ |L - \sqrt{4N}| \sim \mathcal{O}(N^{-1/6}) \\ 1 - \tilde{G}_N(L) & \sim (-1)^N \exp\left[-N \phi_+^B\left(L/\sqrt{4N}\right)\right] \,,\ L > \sqrt{4N} \ \&\ |L - \sqrt{4N}| \sim \mathcal{O}(\sqrt{N}) \,, \end{cases} \tag{22}$$

where $\mathcal{F}_2$ is the TW distribution for GUE, whose explicit expression is given in (1) and its asymptotic behaviors are given in Eq. (5). The rate functions $\phi_\pm^B(x) = \frac{1}{2}\phi_\pm^A(x)$ can be computed

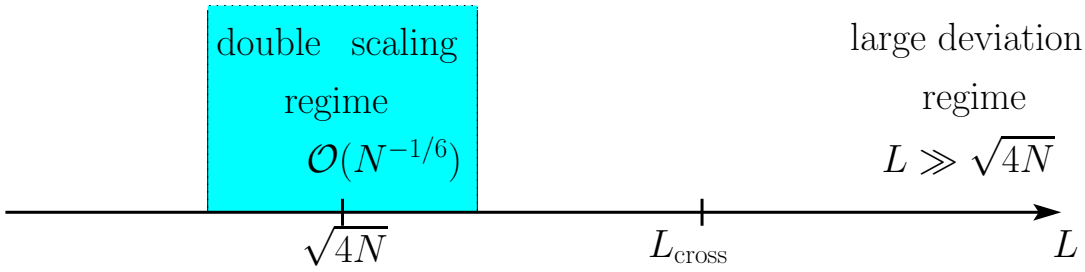

Fig. 3 Crossover from the double scaling to the large deviation regime which occurs only for model B. This crossover happens for $L_{\rm cross} \sim N^{-1/6}(\ln N)^{2/3}$.

exactly (see later). Of particular interest are their asymptotic behaviors when $L \to \sqrt{4N}$ from below (left tail) and from above (right tail), which are given by

$$\phi_-^B(x) \sim \frac{8}{3}(1-x)^3 \ , \ x \to 1^- \ , \tag{23}$$
$$\phi_+^B(x) \sim \frac{2^{7/2}}{3}(x-1)^{3/2} \ , \ x \to 1^+ \ .$$

Notice also the oscillating sign in the right tail of $\tilde{G}_N(L)$ in Eq. (22) which is not problematic here as $\tilde{G}_N(L)$ does not have the meaning of a cumulative distribution. As explained before for model A in Eq. (14), the cubic behavior of $\phi_-^B(x)$ when x approaches 1 from below is again the signature of a third order phase transition in this model. On the other hand, by comparing the asymptotic behavior of $\mathcal{F}_2$ in Eq. (5) with the one of the rate functions (23) we can check, in this case of model B, that the expansion of the large deviation functions around the transition point $L = \sqrt{4N}$ coincides with the tail behavior of the TW scaling function, only for the left tail.

Indeed, using the behavior of $\phi_-^B(x)$ in Eq. (23), one finds from Eq. (22) that

$$\tilde{G}_N(L) \sim \exp\left[-\frac{1}{3}N^{1/2}(L-\sqrt{4N})^3\right] \ , \ 1 \ll \sqrt{4N} - L \ll \sqrt{4N} \tag{24}$$

which matches perfectly with the left tail of the central region (5). However, we find that this property does not hold for the right tail. Indeed, using the asymptotic behavior of $\phi_+^B(x)$ in Eq. (23) one finds from (22)

$$1 - \tilde{G}_N(L) \sim (-1)^N \exp\left[-\frac{4}{3}N^{1/4}(L-\sqrt{4N})^{3/2}\right] , 1 \ll L - \sqrt{4N} \ll \sqrt{4N} \tag{25}$$

with an oscillating sign $\propto (-1)^N$. On the other hand the right tail of the central region, described by $\mathcal{F}_2(t)$ in Eq. (5), yields for $L - \sqrt{4N} \gg N^{-1/6}$

$$1 - \tilde{G}_N(L) \sim 1 - \mathcal{F}_2\left[2^{2/3}N^{1/6}(L-\sqrt{4N})\right] \sim \exp\left[-\frac{8}{3}N^{1/4}\left(L-\sqrt{4N}\right)^{3/2}\right] , \tag{26}$$

without any oscillating sign and where the argument of the exponential is twice larger than the one in (25). This mismatching is the sign of an interesting crossover which happens in this case and which we study in detail below. It can be summarized as follows. Close to $L = \sqrt{4N}$, with $L - \sqrt{4N} \sim \mathcal{O}(N^{-1/6})$, a careful computation beyond leading order shows that

$$\ln \tilde{G}_N(L) = \ln \mathcal{F}_2(t) + (-1)^{N-1}N^{-1/3}2^{-1/3}q(t) + \mathcal{O}(N^{-2/3}) \ , \ t = 2^{2/3}N^{1/6}(L-\sqrt{4N}) \ , \tag{27}$$

where $q(t)$ is the Hastings-McLeod solution of PII (2, 3). In the large t limit, these two competing terms $\ln \mathcal{F}_2(t)$ and $q(t)$ in Eq. (27) behave like (3, 5)

$$|\ln \mathcal{F}_2(t)| \sim e^{-\frac{4}{3}t^{3/2}} \ , \ q(t) \sim \mathrm{Ai}(t) \sim e^{-\frac{2}{3}t^{3/2}} \ . \tag{28}$$

Therefore what happens when one increases L from the critical region $L - \sqrt{4N} \sim \mathcal{O}(N^{-1/6})$ towards the large deviation regime in the right tail $L > \sqrt{4N}$ is the following (see Fig. 3): the amplitude of the second term in the right hand side of Eq. (27) which is oscillating with N, increases relatively to the amplitude of the first term. At some crossover value $L \equiv L_{\rm cross}(N)$ it becomes larger than the first one and in the large deviation regime it becomes the leading term, still oscillating with N (22). Balancing these two terms and making use of the above asymptotic behaviors (28) one obtains an estimate of $L_{\rm cross}(N)$ as

$$L_{\rm cross} - \sqrt{4N} \sim N^{-1/6} (\ln N)^{2/3} \ . \tag{29}$$

Note that such a peculiar crossover is absent in the distribution of the largest eigenvalue of GUE random matrices and it is thus a specific feature of this vicious walkers problem.

Model C: We consider a third model of non-intersecting Brownian motions where the walkers move again on a finite line segment $[0, L]$, but this time with *reflecting* boundary conditions at both boundaries 0 and L. This corresponds to N-dimensional Brownian motion in an affine Weyl chamber of type $\tilde{B}_N$ [39,40]. Again the walkers start in the vicinity of the origin at time $\tau = 0$ and we consider the reunion probability $R_L^C(1)$ that they reunite at time $\tau = 1$ at the origin. Following Models A and B, we define the normalized reunion probability

$$\tilde{E}_N(L) = \frac{R_L^C(1)}{R_\infty^C(1)} \ , \tag{30}$$

that is independent of the starting positions $\{\epsilon_1, \epsilon_2, \ldots, \epsilon_N\}$ in the limit when all the ϵ_i's tend to zero and hence depends only on N and L. As shown in Ref. [19], see also in section 3, $\tilde{E}_N(L)$ can be computed exactly as

$$\tilde{E}_N(L) = \frac{C_N}{L^{2N^2-N}} \sum_{n_1=-\infty}^{\infty} \cdots \sum_{n_N=-\infty}^{\infty} \Delta^2(n_1^2, \ldots, n_N^2) e^{-\frac{\pi^2}{2L^2}\sum_{j=1}^N n_j^2} \ , \tag{31}$$

where $\Delta_N(y_1, \cdots, y_N)$ is the Vandermonde determinant (58) and the prefactor C_N is given by

$$C_N = \frac{\pi^{2N^2-N}\, 2^{N/2-N^2}}{\prod_{j=0}^{N-1} \Gamma(2+j)\Gamma(1/2+j)} \ , \tag{32}$$

which ensures that $\tilde{E}_N(L \to \infty) = 1$. In Ref. [19] we showed that $\tilde{E}_N(L)$, up to a prefactor, is exactly identical to the partition function of the 2-d Yang-Mills theory on a sphere with gauge group SO($2N$):

$$\tilde{E}_N(L) \propto \mathcal{Z}\left(A = \frac{2\pi^2}{L^2} N, \mathrm{SO}(2N)\right) \ . \tag{33}$$

This partition function $\mathcal{Z}\left(A, \mathrm{SO}(2N)\right)$ exhibits the Douglas-Kazakov third order phase transition for $A = \pi^2$ which means that in that case the transition between the right tail and the left tail behavior of $\tilde{E}_N(L)$ occurs for $L = L_c(N) = \sqrt{2N}$. In this paper, we provide a detailed analysis of

the various regimes, right tail, central part and left tail of $\tilde{E}_N(L)$. Our results can be summarized as follows

$$\begin{cases} \tilde{E}_N(L) & \sim \exp\left[-N^2\phi_-^C\left(L/\sqrt{2N}\right)\right] \ , \ L < \sqrt{2N} \ \& \ |L-\sqrt{2N}| \sim \mathcal{O}(\sqrt{N}) \\ \tilde{E}_N(L) & \sim \dfrac{\mathcal{F}_2(s)}{\mathcal{F}_1(s)} \ , \ s = 2^{11/6}N^{1/6}(L-\sqrt{2N}) \ , \ L \sim \sqrt{2N} \ \& \ |L-\sqrt{2N}| \sim \mathcal{O}(N^{-1/6}) \\ 1-\tilde{E}_N(L) & \sim -\exp\left[-N\phi_+^C\left(L/\sqrt{2N}\right)\right] \ , \ L > \sqrt{2N} \ \& \ |L-\sqrt{2N}| \sim \mathcal{O}(\sqrt{N}) \ , \end{cases} \tag{34}$$

where $\mathcal{F}_2$ is the TW distribution for GUE and $\mathcal{F}_1$ the TW distribution for GOE, whose explicit expressions are given in (1, 4) and their asymptotic behaviors are given in Eq. (5). The rate functions $\phi_\pm^C(x) = \phi_\pm^A(x)$ can be computed exactly (see below): their asymptotic behaviors are given in Eq. (13). As explained before for model A in Eq. (14), the cubic behavior of $\phi_-^C(x)$ when x approaches 1 from below is again the signature of a third order phase transition in this model. Similarly, as in the case of model A, we can check that the expansion of the large deviation functions around the transition point $L = \sqrt{2N}$ coincides with the tail behaviors of the central region both in the left tail

$$\tilde{E}_N(L) \sim -\exp\left(-\frac{2^{5/2}}{3}N^{1/2}(\sqrt{2N}-L)^3\right) \ , \ 1 \ll \sqrt{2N}-L \ll \sqrt{2N} \ , \tag{35}$$

as well as in the right tail

$$1-\tilde{E}_N(L) \sim -\exp\left(-\frac{2^{15/4}}{3}N^{1/4}(L-\sqrt{2N})^{3/2}\right) \ , \ 1 \ll L-\sqrt{2N} \ll \sqrt{2N} \ , \tag{36}$$

where, here again, the minus sign is not problematic as $\tilde{E}_N(L)$ does not have the interpretation of a cumulative probability distribution.

3 Derivation of the formula for the reunion probabilities

In this section, we derive the expressions of the normalized reunion probabilities given in Eqs. (7, 19, 31). The derivations are based on a Fermionic path integral method. For model A, this result was first reported in Ref. [12].

3.1 Model A: absorbing boundary conditions at $x = 0$ and $x = L$

We start by the computation of $\tilde{F}_N(L)$ defined in Eq. (6). It then follows that

$$\tilde{F}_N(L) = \lim_{\epsilon_i \to 0}\left[\frac{N(\boldsymbol{\epsilon}, L)}{N(\boldsymbol{\epsilon}, L\to\infty)}\right] \ , \tag{37}$$

where we use the notation $\boldsymbol{\epsilon} \equiv \epsilon_1, \cdots, \epsilon_N$ and where $N(\boldsymbol{\epsilon}, L)$ is the probability that the N Brownian paths, with diffusion coefficient $D = 1/2$, starting at $0 < \epsilon_1 < \cdots < \epsilon_N$ at $\tau = 0$ come back to the same points at $\tau = 1$ without crossing each other and staying within the interval $[0, L]$, with absorbing boundary conditions at $x = 0$ and $x = L$.

To proceed, let us first consider the simple case of N *independent* and free Brownian walkers on a line, each with diffusion constant $D = 1/2$, over the unit time interval $[0, 1]$, *but without*

the non-intersection constraint. The probability measure of an assembly of N trajectories, that start at $\boldsymbol{\epsilon}$ and also end at $\boldsymbol{\epsilon}$, would then be simply proportional to the propagator

$$P_{\text{free}}\left(\boldsymbol{\epsilon},\tau=0|\boldsymbol{\epsilon},\tau=1\right)=\int\mathcal{D}x_i(\tau)\exp\left[-\frac{1}{2}\sum_{i=1}^{N}\int_0^1\left(\frac{dx_i}{d\tau}\right)^2d\tau\right]\prod_{i=1}^{N}\delta[x_i(0)-\epsilon_i]\delta[x_i(1)-\epsilon_i]\;. \tag{38}$$

If, in addition, we subject the walkers to stay within the box $[0,L]$ during the time interval $[0,1]$, this is equivalent to putting an infinite potential at the two ends of the box $[0,L]$. Then one can use path integral techniques to write $N(\boldsymbol{\epsilon},L)$ as the propagator

$$N(\boldsymbol{\epsilon},L)=\langle\boldsymbol{\epsilon}|e^{-\hat{H}_L}|\boldsymbol{\epsilon}\rangle\;,\;H_L=\sum_{i=1}^{N}\left[-\frac{1}{2}\frac{\partial^2}{\partial x_i^2}+V_L(x_i)\right]\;, \tag{39}$$

where $V_L(x)$ is a confining potential with

$$V_L(x)=\begin{cases}0\;,\;x\in[0,L]\;,\\+\infty\;,\;x\notin[0,L]\;.\end{cases} \tag{40}$$

If one denotes by E the eigenvalues of $\hat{H}_L$ (39) and $|E\rangle$ the corresponding eigenvectors, one has

$$N(\boldsymbol{\epsilon},L)=\sum_E|\Psi_E(\boldsymbol{\epsilon})|^2e^{-E}\;,\;\Psi_E(\boldsymbol{\epsilon})=\langle\boldsymbol{\epsilon}|E\rangle\;. \tag{41}$$

So far, we have not implemented the *non-intersection* constraint. The important observation that we make is that this constraint can be incorporated within the path integral framework by simply insisting that the many body wave function $\Psi_E(\boldsymbol{x})\equiv\Psi_E(x_1,\cdots,x_N)$ must be Fermionic, i.e. it vanishes if any of the two coordinates are equal. This many-body antisymmetric wave function is thus constructed from the one-body eigenfunctions of $\hat{H}_L$ by forming the associated Slater determinant. In the case of model A, we note that the single particle wave-functions vanishing at $x=0$ and $x=L$ are

$$\phi_n(x)=\sqrt{\frac{2}{L}}\sin\left(\frac{n\pi x}{L}\right)\;,\;n\in\mathbb{Z}^+\;, \tag{42}$$

such that the eigenfunctions $\Psi_E(\boldsymbol{\epsilon})$ and eigenvalues E in Eq. (41) are given here by

$$\Psi_E(\boldsymbol{\epsilon})=\frac{1}{\sqrt{N\,!}}\det_{1\le i,j\le N}\phi_{n_i}(\epsilon_j)\;,\;E=\frac{\pi^2}{2L^2}\sum_{i=1}n_i^2\;. \tag{43}$$

Hence one has

$$N(\boldsymbol{\epsilon},L)=\frac{1}{N!}\left(\frac{2}{L}\right)^N\sum_{n_1=1}^{\infty}\cdots\sum_{n_N=1}^{\infty}\left|\begin{matrix}\sin\left(\frac{n_1\pi\epsilon_1}{L}\right)&\sin\left(\frac{n_1\pi\epsilon_2}{L}\right)&\cdots&\sin\left(\frac{n_1\pi\epsilon_N}{L}\right)\\\sin\left(\frac{n_2\pi\epsilon_1}{L}\right)&\sin\left(\frac{n_2\pi\epsilon_2}{L}\right)&\cdots&\sin\left(\frac{n_2\pi\epsilon_N}{L}\right)\\\cdot&\cdot&\cdot&\cdot\\\cdot&\cdot&\cdot&\cdot\\\sin\left(\frac{n_N\pi\epsilon_1}{L}\right)&\sin\left(\frac{n_N\pi\epsilon_2}{L}\right)&\cdots&\sin\left(\frac{n_N\pi\epsilon_N}{L}\right)\end{matrix}\right|^2e^{-\frac{\pi^2}{2L^2}\sum_{i=1}^{N}n_i^2} \tag{44}$$

We now have to study the limit of $N(\boldsymbol{\epsilon}, L)$ in Eq. (44) when $\epsilon_i \to 0$ ($\forall i = 1, \cdots, N$). One can then check that to leading order, one has

$$\begin{vmatrix} \sin\left(\frac{n_1\pi\epsilon_1}{L}\right) & \sin\left(\frac{n_1\pi\epsilon_2}{L}\right) & \cdots & \sin\left(\frac{n_1\pi\epsilon_N}{L}\right) \\ \sin\left(\frac{n_2\pi\epsilon_1}{L}\right) & \sin\left(\frac{n_2\pi\epsilon_2}{L}\right) & \cdots & \sin\left(\frac{n_2\pi\epsilon_N}{L}\right) \\ \cdot & \cdot & \cdot & \cdot \\ \cdot & \cdot & \cdot & \cdot \\ \sin\left(\frac{n_N\pi\epsilon_1}{L}\right) & \sin\left(\frac{n_N\pi\epsilon_2}{L}\right) & \cdots & \sin\left(\frac{n_N\pi\epsilon_N}{L}\right) \end{vmatrix}^2 \sim \frac{a_1}{L^{2N^2}} \left[\prod_{i=1}^N n_i^2 \prod_{i<j} (n_i^2 - n_j^2)^2\right] \left[\prod_{i=1}^N \epsilon_i^2 \prod_{i<j} (\epsilon_i^2 - \epsilon_j^2)^2\right], \tag{45}$$

where a_1 is a numerical constant independent of n_i's and ϵ_i's. Therefore one obtains

$$\tilde{F}_N(L) = \frac{a_2}{L^{2N^2+N}} \lim_{\epsilon_i \to 0} \left[\frac{\prod_{i=1}^N \epsilon_i^2 \prod_{i<j} (\epsilon_i^2 - \epsilon_j^2)^2}{N(\boldsymbol{\epsilon}, L \to \infty)}\right] \sum_{n_1=1}^{\infty} \cdots \sum_{n_N=1}^{\infty} \prod_{i=1}^N n_i^2 \prod_{i<j} (n_i^2 - n_j^2)^2 e^{-\frac{\pi^2}{2L^2} \sum_{i=1}^N n_i^2}, \tag{46}$$

with $a_2 = 2^N a_1$. To compute $N(\boldsymbol{\epsilon}, L \to \infty)$, starting from Eq. (44) one first notices that the product of determinants can be replaced by the same limiting behavior as in the $\epsilon_i \to 0$ limit given in Eq. (45) as this product is a function of the variables ϵ_i/L's only. One can then perform the remaining multiple sums over n_i's in (44) by noticing that they can be replaced by integrals in the limit $L \to \infty$ – as done below in Eq. (50). Finally, one obtains that

$$\lim_{\epsilon_i \to 0} \left[\frac{\prod_{i=1}^N \epsilon_i^2 \prod_{i<j} (\epsilon_i^2 - \epsilon_j^2)^2}{N(\boldsymbol{\epsilon}, L \to \infty)}\right] = a_3 , \tag{47}$$

where a_3 is a constant independent of L. Therefore, combining these results (46, 47), and using the symmetry of the summand in Eq. (46) under the transformation $n_i \to -n_i$, one arrives at

$$\tilde{F}_N(L) = \frac{A_N}{L^{2N^2+N}} \sum_{n_1=-\infty}^{\infty} \cdots \sum_{n_N=-\infty}^{\infty} \prod_{i=1}^N n_i^2 \prod_{i<j} (n_i^2 - n_j^2)^2 e^{-\frac{\pi^2}{2L^2} \sum_{i=1}^N n_i^2} , \tag{48}$$

as announced before (7), where the constant A_N remains however undetermined. It can be computed using the normalization condition of $\tilde{F}_N(L)$ which follows directly from its definition (6)

$$\lim_{L \to \infty} \tilde{F}_N(L) = 1 . \tag{49}$$

Indeed, as we mentioned it above, in the limit when $L \to \infty$, the discrete variables $\pi n_i/L \equiv k_i$ which naturally enter into the expression of $\tilde{F}_N(L)$ in Eq. (48) become continuous variables. Therefore the discrete sums in Eq. (48) can be replaced by integrals in the $L \to \infty$ limit, giving

$$\lim_{L \to \infty} \tilde{F}_N(L) = \frac{A_N}{\pi^{2N^2+N}} \int_{-\infty}^{\infty} dk_1 \cdots \int_{-\infty}^{\infty} dk_N \prod_{i=1}^N k_i^2 \prod_{i<j} (k_i^2 - k_j^2)^2 e^{-\frac{1}{2} \sum_{i=1}^N k_i^2} . \tag{50}$$

If one restricts the integrals over $k_i \in [0, +\infty)$ and performs the change of variable $x_i = k_i^2/2$ one obtains

$$\lim_{L \to \infty} \tilde{F}_N(L) = \frac{A_N}{\pi^{2N^2+N}} 2^{N^2+N/2} \int_0^{\infty} dx_1 \cdots \int_0^{\infty} dx_N \prod_{i=1}^N x_i^{1/2} \prod_{i<j} (x_i - x_j)^2 e^{-\sum_{i=1}^N x_i} , \tag{51}$$

where the integral can now be evaluated using a limiting case of the Selberg integral [64]:

$$\int_0^{\infty} dx_1 \cdots \int_0^{\infty} dx_N \prod_{i<j} (x_i - x_j)^{2\gamma} \prod_{i=1}^N x_i^{\alpha-1} e^{-x_i} = \prod_{j=0}^{N-1} \frac{\Gamma(1 + \gamma + j\gamma)\Gamma(\alpha + \gamma j)}{\Gamma(1 + \gamma)} , \tag{52}$$

yielding (with $\gamma = 1$ and $\alpha = 3/2$), the formula for A_N given in Eq. (9), [see also Eq. (59)].

3.2 Model B: periodic boundary conditions

Here we consider N non-intersecting Brownian motions with diffusion coefficient $D = 1/2$ on a line segment $[0, L]$ with periodic boundary conditions or equivalently on a circle of radius $L/2\pi$, starting in the vicinity of the origin at time $\tau = 0$. In this case, the computation of the ratio of reunion probability in Eq. (19) can be done along the same line as before, (39-43). In this case, the positions of the particles are more naturally labelled by their angles θ_i's (rather than their positions x_i's), in terms of which the Hamiltonian $\hat{H}_L$ (39) associated to this diffusion reads (see [19])

$$\hat{H}_L = -\frac{2\pi^2}{L^2} \sum_{i=1}^{N} \frac{\partial^2}{\partial \theta_i^2} \, , \tag{53}$$

which actually comes from the expression of the bi-dimensional Laplacian in terms of polar variables (we recall that the radius of the circle is $L/2\pi$ and the diffusion coefficient is $D = 1/2$). It is easy to see that the one particle eigenfunctions of (53) $\phi_n(\theta)$ which satisfy the boundary conditions $\phi_n(\theta) = \phi_n(\theta + 2\pi)$ are given by

$$\phi_n(\theta) = \frac{1}{\sqrt{2\pi}} e^{in\theta} \, , n \in \mathbb{N} \, , \tag{54}$$

such that the N particle anti-symmetric eigenfunctions $\Psi_E(\boldsymbol{\theta})$ and associated eigenvalues E are given by [see Eq. (43)]

$$\Psi_E(\boldsymbol{\theta}) = \frac{1}{\sqrt{N!}} \det_{1 \leq j,k \leq N} \left[\phi_{n_j}(\theta_k) \right] \, , \; E = \frac{2\pi^2}{L^2} \sum_{i=1}^{N} {n_i}^2 \, . \tag{55}$$

After some manipulations similar to the one performed before in the case of model A, one arrives straightforwardly at the formula for $\tilde{G}_N(L)$ given in Eq. (19).

3.3 Model C: reflecting boundary conditions at $x = 0$ and $x = L$

In this case we consider N non-intersecting Brownian motions with diffusion coefficient $D = 1/2$ on the segment $[0, L]$ with reflecting boundary conditions both at $x = 0$ and $x = L$. The analysis is then exactly the same as the one performed for model A in Eqs. (39)-(43) except that in that case the single particle eigenfunctions $\phi_n(x)$ must satisfy: $\partial_x \phi_n(x) = 0$ at $x = 0$ and $x = L$. It is then easy to see that they are given by

$$\phi_n(x) = \sqrt{\frac{2}{L}} \cos\left(\frac{n\pi x}{L}\right) . \tag{56}$$

After some manipulations, exactly similar to the one performed in the case of model A, one obtains the formula for $\tilde{E}_N(L)$ given in Eq. (31).

In the following sections 4, 5, 6, we analyze these formula (7, 19, 31) in the limit of large N.

4 Large N analysis of the maximal height of N non-intersecting excursions

In this section, we focus on the distribution of the maximal height of N non-intersecting excursions $\tilde{F}_N(L)$ given by

$$\tilde{F}_N(L) = \frac{A_N}{L^{2N^2+N}} \sum_{n_1=-\infty}^{\infty} \cdots \sum_{n_N=-\infty}^{\infty} \prod_{i=1}^{N} n_i^2 \, \Delta_N^2(n_1^2, \cdots, n_N^2) e^{-\frac{\pi^2}{2L^2} \sum_{i=1}^N n_i^2} \, , \tag{57}$$

where $\Delta_N(y_1, \cdots, y_N)$ is the Vandermonde determinant

$$\Delta_N(y_1, \cdots, y_N) = \prod_{1 \le j < k \le N} (y_j - y_k) \, , \tag{58}$$

and the amplitude A_N is given by

$$A_N = \frac{\pi^{2N^2+N}}{2^{N^2+\frac{N}{2}} \prod_{j=0}^{N-1} \Gamma(2+j)\Gamma(\frac{3}{2}+j)} \, . \tag{59}$$

We introduce the parameter α defined as

$$\alpha = \frac{\pi^2}{2L^2} \, , \tag{60}$$

such that $\tilde{F}_N(L)$ can be written as

$$\tilde{F}_N(L) = \frac{1}{\prod_{j=0}^{N-1} \Gamma(2+j)\Gamma(\frac{3}{2}+j)} \alpha^{N^2+\frac{N}{2}} \Omega(\alpha, N) \, , \tag{61}$$

$$\Omega(\alpha, N) = \sum_{n_1=-\infty}^{\infty} \cdots \sum_{n_N=-\infty}^{\infty} \prod_{i=1}^{N} n_i^2 \, \Delta_N^2(n_1^2, \cdots, n_N^2) e^{-\alpha \sum_{i=1}^N n_i^2} \, . \tag{62}$$

The goal of this section is to provide the large N asymptotic analysis of this formula (61, 62). In the large N limit, the leading contribution to $\tilde{F}_N(L)$ comes from $L \sim \mathcal{O}(\sqrt{N})$, and hence $\alpha = \pi^2/(2L^2) \ll 1$. It is thus natural to approximate the multiple sum in $\Omega(\alpha, N)$ (62) by a multiple integral and then evaluate this multiple integral, in the large N limit, using a saddle point method. This saddle point method yields a non trivial result for $L < \sqrt{2N}$, i.e. for the left tail of the distribution, and it will be analyzed in subsection 4.1. This calculation was done for YM_2 with the gauge group $G = \mathrm{U}(N)$ by Douglas and Kazakov [29] and we show below that, after simple manipulations, this saddle point analysis in the present case where $G = \mathrm{Sp}(2N)$ can be achieved without any additional calculation, by borrowing the results of Ref. [29]. On the other hand, for $L > \sqrt{2N}$, the saddle point result for $\Omega(\alpha, N)$ in Eq. (62) compensates exactly, to leading order, the large N behavior of the prefactor $\alpha^{N^2+\frac{N}{2}} / \prod_{j=0}^{N-1} \Gamma(2+j)\Gamma(\frac{3}{2}+j)$ in Eq. (61). Hence for $L > \sqrt{2N}$ the net result of this saddle point analysis is simply $\tilde{F}_N(L) = 1$. The analysis beyond this leading (and trivial) order requires the calculation of non-perturbative, instanton-like, contributions to the partition function. This was first done by Gross and Matytsin [30] in the case of the gauge group $G = \mathrm{U}(N)$, and then by Crescimanno, Naculich and Schnitzer [31] for other gauge groups including $G = \mathrm{Sp}(2N)$, using the method of discrete orthogonal polynomials. We describe this powerful method in subsection 4.2, which then allows us to analyze the right tail of $\tilde{F}_N(L)$ in subsection 4.3. Finally, this method of orthogonal polynomials also allows us to analyze the central part of $\tilde{F}_N(L)$, which describes the typical fluctuations of the maximal height, by studying this system of orthogonal polynomials in the double scaling limit, which is done in subsection 4.4.

4.1 Coulomb gas analysis for large N and the left tail

Physically, it is natural to consider the expression of $\Omega(\alpha, N)$ in Eq. (62) as the partition function of a discrete Coulomb gas. The large N analysis can then be performed along the line of the work of Douglas and Kazakov in the context of the partition function of the YM_2 with the U(N) gauge group [29], using a constrained saddle point analysis. As we show below, although the discrete partition sum $\Omega(\alpha, N)$ in our model is not exactly the same as that of Douglas and Kazakov, it is nevertheless possible to transform directly their result to our case without any further additional work. This then allows us to obtain the left tail of the distribution $\tilde{F}_N(L)$ in the large N limit.

For this purpose we first rewrite $\tilde{F}_N(L)$ in a slightly different way

$$\tilde{F}_N(L) = \frac{2^N}{\prod_{j=0}^{N-1} \Gamma(2+j)\Gamma(\frac{3}{2}+j)} \alpha^{N^2+\frac{N}{2}} \tilde{\Omega}(\alpha, N) \; , \tag{63}$$

$$\tilde{\Omega}(\alpha, N) = \sum_{n_1=0}^{\infty} \cdots \sum_{n_N=0}^{\infty} \prod_{i=1}^{N} n_i^2 \, \Delta_N^2(n_1^2, \cdots, n_N^2) \, e^{-\alpha \sum_{i=1}^N n_i^2} \; , \tag{64}$$

where the integers n_i are then all positive $n_i > 0$ and recall that $\alpha = \pi^2/2L^2$. We now regard the summand in Eq. (64) as a function of the variables

$$x_i = \frac{n_i}{2N} \text{ with } i = 1, \cdots, N \; . \tag{65}$$

In the large N limit the variables $\{n_i/(2N)\}_{i=1,\cdots,N}$ approximate the coordinates of a continuous N particles system and associated with the particles is a density $\tilde{\rho}(x)$. Because of the Vandermonde determinant these particles experience hard core repulsion and behave as fermions. The configuration with highest density corresponds to the case where $n_1 = 1, n_2 = 2, \cdots, n_N = N$ for which the local density is uniform and given by $\tilde{\rho}_{\max} = 2$, the lattice spacing being $1/(2N)$. Therefore the density $\tilde{\rho}(x)$ must satisfy the constraint

$$\tilde{\rho}(x) = \frac{1}{N} \sum_{i=1}^{N} \langle \delta(x - x_i) \rangle \leq 2 \; , \; \int_0^a dx \, \tilde{\rho}(x) = 1 \; , \tag{66}$$

where the average $\langle \cdots \rangle$ is taken with respect to the discrete weight in Eqs. (63, 64) and where $[0, a]$ is thus the support of the mean density, a remaining to be determined.

The main idea is that in the large N limit the discrete sum can be replaced by a multiple integral over continuous variables and this multiple integral can be viewed as the partition function of a Coulomb gas with $x_i = n_i/2N$ denoting the position of the i-th charge. The next step is to replace this multiple integral over N variables by a functional integral over the coarse grained density $\tilde{\rho}(x)$ à la Dyson [61–63] (for a review see Refs. [34,64]). Skipping details, one finds that in terms of the scaling variable

$$h = \frac{L}{\sqrt{2N}} \; , \tag{67}$$

one can approximate to leading order in the large N limit,

$$\tilde{F}_N(h\sqrt{2N}) \sim \int \mathcal{D}\tilde{\rho}(x) e^{-N^2 S[\tilde{\rho}]} \; , \tag{68}$$

$$S[\tilde{\rho}] = \frac{\pi^2}{h^2} \int_0^a dx x^2 \tilde{\rho}(x) - \int_0^a dx \int_0^a dx' \tilde{\rho}(x)\tilde{\rho}(x') \ln|x^2 - x'^2| + C \left[\int_0^a \tilde{\rho}(x) \, dx - 1 \right] \tag{69}$$

where C is a Lagrange multiplier that enforces the normalization condition of the charge density. If we introduce $\rho(x) = \tilde{\rho}(x)/2$, for $x > 0$ and $\rho(x) = \tilde{\rho}(-x)/2$ for $x < 0$ it is easy to see that

$$S[\tilde{\rho}] = 2S_{DK}[\rho] \tag{70}$$

$$S_{DK}[\rho] = \frac{\pi^2}{2h^2}\int_{-a}^{a} dx x^2\rho(x) - \int_{-a}^{a} dx \int_{-a}^{a} dx' \rho(x)\rho(x') \ln|x-x'| + C'\left[\int_{-a}^{a}\rho(x)dx - 1\right] \tag{71}$$

where $C' = C/2$ is a constant and $S_{DK}[\rho]$ is exactly the action studied by Douglas and Kazakov [29] with the substitution $h^2 = \pi^2/A$.

In the large N limit, the path integral over $\tilde{\rho}$ in Eq. (68) can be evaluated by the saddle point method, giving

$$\int \mathcal{D}\tilde{\rho}(x) e^{-N^2 S[\tilde{\rho}]} \sim \exp\left(-2N^2 S_{DK}[\rho^*]\right) , \tag{72}$$

where ρ^* is such that

$$\left.\frac{\delta S_{DK}[\rho]}{\delta\rho(x)}\right|_{\rho=\rho^*} = 0 , \tag{73}$$

which gives an integral equation for the saddle point density

$$\frac{\pi^2}{2h^2}\, x^2 - 2\int_{-a}^{a} \rho^*(x') \ln|x-x'|\, dx' + C' = 0 \tag{74}$$

that holds only over the support $x \in [-a, a]$ where $\rho^*(x)$ is nonzero. Taking a further derivative with respect to x gets rid of the Lagrange multiplier C' and leads to a singular integral equation for $\rho^*(x)$

$$\frac{\pi^2}{2h^2} x - \fint_{-a}^{a} \frac{\rho^*(x')}{x-x'} dx' = 0 , \tag{75}$$

where $\fint$ stands for the principal part of the integral, together with the constraints on $\rho(x)$, inherited from the ones on $\tilde{\rho}$ in Eq. (66)

$$\int_{-a}^{a} \rho^*(x)dx = 1 \ , \ \rho^*(x) \leq 1 \ , \forall x \in [-a, a] . \tag{76}$$

If one first discards the constraint $\rho^*(x) \leq 1$, the solution of the saddle point equation (75) is simply given by the Wigner semi-circle law [64]

$$\rho^*(x) = \frac{\pi}{2h^2}\sqrt{\frac{4h^2}{\pi^2} - x^2} , \tag{77}$$

and thus $a = 2h/\pi$. This density $\rho^*(x)$ has its maximum at $x = 0$, where $\rho^*(0) = 1/h$: therefore the Wigner semi-circle law is the solution of this constrained saddle point equation as long as $h > 1$. Noting that $h = L/\sqrt{2N} > 1$ means $L > \sqrt{2N}$, this solution then corresponds to the right tail of the distribution $\tilde{F}_N(L)$ (see Fig. 4).

What happens when $h < 1$, or equivalently $L < \sqrt{2N}$? Clearly, the Wigner semi-circle is no longer the right solution since it violates the constraint $\rho^*(x) \leq 1$. So, there must be another solution to the singular integral equation when $h < 1$. When h approaches 1 from above, the maximum of the semi-circle at $x = 0$ just touches 1. As one decreases h below 1, the density at $x = 0$ cannot obviously increase beyond 1 since its maximum value is 1. What happens instead

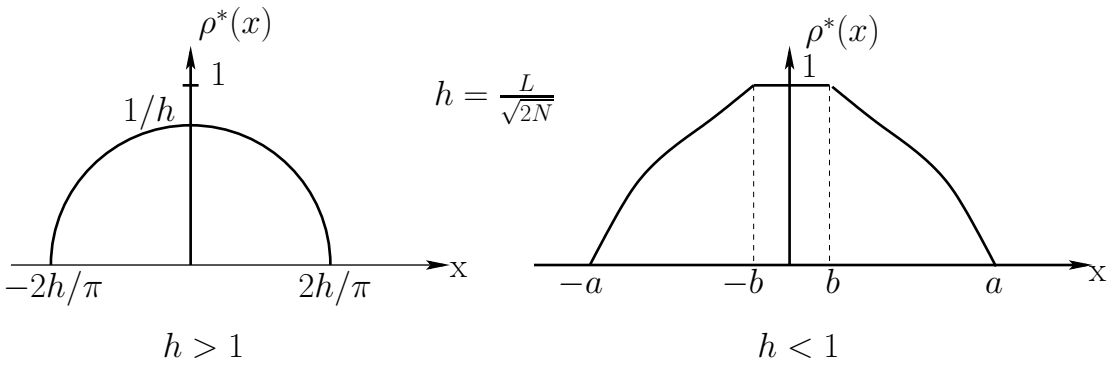

$h > 1$ $h < 1$

Fig. 4 Sketch of the density $\rho^*(x)$ for $h < 1$ (left tail), and $h > 1$ (right tail). The Douglas-Kazakov transition occurs for $h = 1$, when $L = L_c(N) = \sqrt{2N}$ in model A, where $\rho^*(0) = 1$.

is like a 'wetting' transition, i.e., the density becomes flat and equal to 1 symmetrically around $x = 0$ over an interval $[-b, b]$ and outside the interval it has a nontrivial shape (see the right panel of Fig. 4). In other words, the solution reads

$$\rho^*(x) = 1 \, , x \in [-b, b] \, , \rho^*(x) = \hat{\rho}(x) \; , \; x \in [-a, -b] \cup [a, b] \; , \tag{78}$$

where $\hat{\rho}(x)$ is non zero only for $x \in [-a, -b] \cup [a, b]$. Substituting this ansatz in Eq. (75) provides an integral equation for the nontrivial part $\hat{\rho}(x)$ of the density

$$\frac{\pi^2}{2h^2} x - \ln\left(\frac{x-b}{x+b}\right) - \int_{-a}^{a} \frac{\hat{\rho}(x')}{x - x'} dx' = 0 \; . \tag{79}$$

Note that both a and b have to be self-consistently determined. This integral equation for $\hat{\rho}$ can be solved explicitly in terms of elliptic functions [29] (here we give the expression from Ref. [65]):

$$\hat{\rho}(x) = \frac{2}{\pi a x} \sqrt{(a^2 - x^2)(x^2 - b^2)} \Pi_1\left(-\frac{b^2}{x^2}, \frac{b}{a}\right) \; , \; x \in [-a, -b] \cup [a, b] \; , \tag{80}$$

where $\Pi_1(y, k)$ is the elliptic integral of the third kind, which admits the following integral representation

$$\Pi_1(y, k) = \frac{1}{2} \int_{-1}^{1} \frac{dz}{1 + y\, z^2} \frac{1}{\sqrt{1 - k^2 z^2}\sqrt{1 - z^2}} \; . \tag{81}$$

The constants a and b in Eqs (78, 80) can be expressed in terms of standard elliptic integrals (using the notations of Ref. [66])

$$\mathbf{K}(y) = \int_0^1 \frac{dz}{\sqrt{1 - y^2 z^2}\sqrt{1 - z^2}} \; , \; \mathbf{E}(y) = \int_0^1 dz \frac{\sqrt{1 - y^2 z^2}}{1 - z^2} \; . \tag{82}$$

Then a and b are determined by the following relations

$$k = \frac{b}{a} \tag{83}$$

$$a[2\mathbf{E}(k) - (1 - k^2)\mathbf{K}(k)] = 1 \tag{84}$$

$$a \frac{\pi^2}{h^2} = 4\mathbf{K}(k) \; . \tag{85}$$

Reverting back to our original problem, described by the action $S[\tilde{\rho}]$ in Eq. (68), with $\tilde{\rho}(x) = 2\rho(x)$, we get that the saddle point is obtained for $\tilde{\rho}(x) = \tilde{\rho}^*(x)$ where, for $h > 1$,

$$\tilde{\rho}^*(x) = \begin{cases} 0 \ , \ x < 0 \\ \dfrac{\pi}{h^2}\sqrt{\dfrac{4h^2}{\pi^2} - x^2} \ , \ 0 \leq x \leq \dfrac{2h}{\pi} \\ 0 \ , \ x > \dfrac{2h}{\pi} \end{cases} \tag{86}$$

while for $h < 1$ one has

$$\tilde{\rho}^*(x) = \begin{cases} 0 \ , \ x < 0 \\ 2 \ , \ 0 \leq x \leq b \\ \dfrac{4}{\pi a x}\sqrt{(a^2 - x^2)(x^2 - b^2)}\Pi_1\left(-\dfrac{b^2}{x^2}, \dfrac{b}{a}\right) \ , \ b \leq x \leq a \\ 0 \ , \ x > a \ . \end{cases} \tag{87}$$

These explicit expressions for $\rho^*(x)$ given in Eq. (77) for $h > 1$ and in Eqs. (78, 80) for $h < 1$ can then be plugged into Eq. (72) as done in Ref. [29] to obtain

$$\lim_{N\to\infty} -\frac{1}{N^2}\ln \tilde{F}_N(h\sqrt{2N}) = \begin{cases} 0 \ , \ h \geq 1 \\ \phi_A^-(h) = 2\left(F_-(\pi^2/h^2) - F_+(\pi^2/h^2)\right) \ , \ h < 1 \ , \end{cases} \tag{88}$$

where

$$F_-(X) = -\frac{3}{4} - \frac{X}{24} - \frac{1}{2}\ln X \ , \tag{89}$$

while $F_+(X)$ has a more complicated, though explicit, expression in terms of elliptic integrals:

$$F'_+(X) = \frac{a^2}{6} - \frac{a^2}{12}(1-k^2) - \frac{1}{24} + \frac{a^4}{96}(1-k^2)^2 X \ , \tag{90}$$

where a and k are defined by the relations in Eqs. (83)-(85) with the substitution, in the last relation (85) $\pi^2/h^2 \to X$. This result in Eq. (88) yields the expression of the left tail of $\tilde{F}_N(L)$ announced in the section 2 in Eq. (12).

The result of this Coulomb gas approach in Eq. (88) indicates that this quantity $\tilde{F}_N(L)$ exhibits a phase transition at $h = 1$, i.e. at $L = L_c(N) = \sqrt{2N}$. To investigate the order of this transition, we need to analyze the behavior of the rate function $\phi_A^-(h)$ in Eq. (88) when $h \to 1$, which requires the behavior of $F_-(X) - F_+(X)$ for X close to π^2, which was computed in Ref. [29] as [1]

$$F_-(X) - F_+(X) = \frac{1}{3\pi^6}\left(X - \pi^2\right)^3 + \mathcal{O}((X-\pi^2)^4) \ . \tag{91}$$

This cubic behavior implies a third order phase transition as the third derivative of the rate function presents a discontinuity when h crosses the critical value $h = 1$. Note also that, when $h \to 1$, $h < 1$, one obtains that $\tilde{F}_N(h\sqrt{2N})$ behaves like

$$\tilde{F}_N(h\sqrt{2N}) \sim e^{-N^2 \frac{16}{3}(1-h)^3} \ , \tag{92}$$

which yields the asymptotic behavior of the rate function $\phi_A^-(h)$ given in Eq. (13).

[1] Note that we have corrected a sign error from Ref. [29] and reproduced also in Ref. [19]

We see in Eq. (88) that this saddle point approach does not say anything relevant about the right tail of the distribution. It just gives the trivial leading order result that $\tilde{F}_N(L) \approx 1$ for $L > \sqrt{2N}$. To investigate this regime beyond this trivial leading order, we have to find some other method. Fortunately such a method exists and it involves discrete orthogonal polynomials which were introduced and studied by Gross and Matytsin [30] in the context of YM_2 with the U(N) gauge group. We can adapt their method to our problem as shown in the next subsection. We will see that this method also allows us to study not just the extreme right tail but also the typical fluctuations, for $L \sim \sqrt{2N}$, which is described by a double scaling limit which we analyze below.

4.2 General expression in terms of discrete orthogonal polynomials

To analyze (61, 62) in the large N limit, we follow Ref. [30] and introduce the following discrete orthogonal polynomials

$$\sum_{n=-\infty}^{\infty} p_k(n|\alpha) p_{k'}(n|\alpha) e^{-\alpha n^2} = \delta_{k,k'} h_k(\alpha) \ , \tag{93}$$

where we recall that $\alpha = \pi^2/2L^2$. Here $p_k(n|\alpha)$'s are monic polynomials of degree k:

$$p_k(n|\alpha) = n^k + \cdots \tag{94}$$

and $h_k(\alpha)$'s are to be determined.

These orthogonal polynomials turn out to be very useful as they allow us to express $\tilde{F}_N(L)$ in a rather compact form, as we show now. First notice that

$$\prod_{i=1}^{n} n_i \, \Delta(n_1^2, n_2^2, \cdots, n_N^2) = \det_{1 \le i,j \le N} \left[p_{2i-1}(n_j) \right] \ . \tag{95}$$

Using this in Eq. (62) we get

$$\Omega(\alpha, N) = \sum_{n_1=-\infty}^{\infty} \cdots \sum_{n_N=-\infty}^{\infty} e^{-\alpha \sum_{i=1}^{N} n_i^2} \left[\det_{1 \le i,j \le N} \left[p_{2i-1}(n_j) \right] \right]^2 \ . \tag{96}$$

Next, using the definition in Eq. (93) and the discrete version of the Cauchy-Binet formula one gets

$$\Omega(\alpha, N) = \Gamma(N+1) \prod_{j=1}^{N} h_{2j-1}(\alpha) \ . \tag{97}$$

Thus, if we can determine the $h_k(\alpha)$'s, in principle we can determine $\Omega(\alpha, N)$ exactly.

So, our next task is to determine the $h_k(\alpha)$'s. As we show below, one can actually set up a very nice recursive procedure to determine the $h_k(\alpha)$'s. To proceed, we notice that the two first polynomials are obtained straightforwardly as

$$p_0(n|\alpha) = 1 \ , \ p_1(n|\alpha) = n \ , \tag{98}$$

from which one gets the first amplitudes

$$h_0(\alpha) = \sum_{n=-\infty}^{\infty} e^{-\alpha n^2} \ , \ h_1(\alpha) = \sum_{n=-\infty}^{\infty} n^2 e^{-\alpha n^2} \ . \tag{99}$$

Note that given that the weight $e^{-\alpha n^2}$ is symmetric under the transformation $n \to -n$ and given that the sum in Eq. (93) runs over $n \in \mathbb{Z}$, one can show (for instance by induction over k) that

$$\begin{aligned} p_{2k}(n) &= n^{2k} + a_{2k-2}n^{2k-2} + \cdots + a_0 \\ p_{2k+1}(n) &= n^{2k+1} + b_{2k-1}n^{2k-1} + \cdots + b_1 n \ . \end{aligned} \tag{100}$$

Because p_k's are orthogonal polynomials (93) they satisfy a three term recursion relation [67]:

$$np_k(n|\alpha) = p_{k+1}(n|\alpha) + S_k(\alpha)p_k(n|\alpha) + R_k(\alpha)p_{k-1}(n|\alpha) \ . \tag{101}$$

Multiplying the above recursion relation (101) by $p_k(n|\alpha)e^{-\alpha n^2}$ and summing over n, one obtains from (100) that

$$S_k(\alpha) = 0 \ . \tag{102}$$

On the other hand, multiplying both sides of Eq. (101) by $p_{k-1}(n|\alpha)e^{-\alpha n^2}$ and summing over n one obtains

$$R_k(\alpha) = \frac{h_k(\alpha)}{h_{k-1}(\alpha)} \ . \tag{103}$$

From Eq. (99), one has

$$R_1(\alpha) = \frac{h_1(\alpha)}{h_0(\alpha)} = \frac{\sum_{n=-\infty}^{\infty} n^2 e^{-\alpha n^2}}{\sum_{n=-\infty}^{\infty} e^{-\alpha n^2}} = -\frac{d}{d\alpha} \ln h_0(\alpha) \ . \tag{104}$$

Inspired by the relation found above for $R_1(\alpha)$ (104), we differentiate the orthogonality condition (93) with respect to α

$$\frac{d}{d\alpha}h_k(\alpha) = -\langle np_k|np_k\rangle + 2\langle p_k|\partial_\alpha p_k\rangle \ , \tag{105}$$

where we have introduced the notation $\langle f|g\rangle$, for two functions f, g:

$$\langle f|g\rangle = \sum_{n=-\infty}^{\infty} f(n)g(n)e^{-\alpha n^2} \ . \tag{106}$$

Using the fact that p_k is a monic polynomial (94), $\partial_\alpha p_k$ is thus a polynomial of degree at most $k-2$ (100). And therefore, from the orthogonality condition (93), the second term in (105) vanishes. Finally, using the recursion relation (101) one obtains

$$\frac{d}{d\alpha}h_k(\alpha) = -\left(R_{k+1}(\alpha)h_k(\alpha) + R_k(\alpha)h_k(\alpha)\right) \ . \tag{107}$$

From the relation found above for $R_1(\alpha)$ (104) we see, from Eq. (107) that one has, for consistency:

$$R_0(\alpha) = 0 \ . \tag{108}$$

By subtracting the relations (107) for $\frac{d}{d\alpha}h_k(\alpha)$ and $\frac{d}{d\alpha}h_{k-1}(\alpha)$ one obtains

$$-\frac{d}{d\alpha} \ln R_k(\alpha) = R_{k+1}(\alpha) - R_{k-1}(\alpha) \ . \tag{109}$$

Let us then summarize the main program to be carried out. We have a set of variables $R_k(\alpha)$'s that satisfy a Volterra type recursion relation in Eq. (109), starting from the initial values: $R_0(\alpha) = 0$ and $R_1(\alpha) = -\frac{d}{d\alpha} \ln h_0(\alpha)$ where $h_0(\alpha) = \sum_{n=-\infty}^{\infty} e^{-\alpha n^2}$. This is a closed set of deterministic recursive relations, albeit nonlinear. In principle, if we have the solution $R_k(\alpha)$

for arbitrary k, then we can determine the $h_k(\alpha)$'s by iterating the relation (103): $h_k(\alpha) = R_k(\alpha)h_{k-1}(\alpha)$, starting from $h_0(\alpha) = \sum_{n=-\infty}^{\infty} e^{-\alpha n^2}$. Once we have the $h_k(\alpha)$'s for all k, by taking their product in Eq. (97), we can determine, at least in principle, $\Omega(\alpha, N)$ and hence subsequently $\tilde{F}_N(L)$ using Eq. (61).

Actually, to get rid of the complicated prefactor in Eq. (61), it turns out to be useful to consider the following ratio

$$\frac{\tilde{F}_{N+1}(L)\tilde{F}_{N-1}(L)}{\tilde{F}_N^2(L)} = \frac{\alpha^2}{N(N+1/2)}\frac{h_{2N+1}(\alpha)}{h_{2N-1}(\alpha)} = \frac{\alpha^2}{N(N+1/2)}R_{2N+1}(\alpha)R_{2N}(\alpha) \;, \tag{110}$$

where we have used Eqs. (61), (97) and (103) to simplify. This will turn out to be the most useful form on which one can perform the asymptotic analysis for large N and large L.

So, essentially, our aim and the main challenge are to solve the nonlinear recursion relation for the $R_k(\alpha)$'s in Eq. (109). Evidently, this can not be solved for all k exactly. However, for large k and large L (i.e., small $\alpha = \pi^2/2L^2$), it turns out that one can make some scaling ansatz and solve the resulting differential equation for the scaling functions. This provides us a handle on the asymptotic analysis of $\tilde{F}_N(L)$, as we show below in the next two subsections.

4.3 Large deviation regime: right tail

To begin with, we first consider the limit when $L \to \infty$, *i.e.* $\alpha = \frac{\pi^2}{2L^2} \to 0$, with N fixed to a large value. To get insight into this limit, it is useful to study the amplitudes $h_0(\alpha), h_1(\alpha)$ in Eq. (99) when $\alpha \to 0$. For this purpose, we use the Poisson summation formula: if for a given function $f(x)$ we define its Fourier transform

$$\hat{f}(q) = \frac{1}{2\pi}\int_{-\infty}^{\infty} f(x)e^{iqx}\,dx \;, \tag{111}$$

then one has

$$\sum_{n=-\infty}^{\infty} \hat{f}(n) = \sum_{n=-\infty}^{\infty} f(2\pi n) \;. \tag{112}$$

When applied to $h_0(\alpha)$ and $h_1(\alpha)$ this Poisson formula yields

$$h_0(\alpha) = \sqrt{\frac{\pi}{\alpha}}\sum_{n=-\infty}^{\infty} e^{-\frac{\pi^2 n^2}{\alpha}} = \sqrt{\frac{\pi}{\alpha}}\left(1 + 2\,e^{-\frac{\pi^2}{\alpha}} + \mathcal{O}(e^{-\frac{4\pi^2}{\alpha}})\right) \;, \tag{113}$$

$$h_1(\alpha) = \frac{\sqrt{\pi}}{2\alpha^{\frac{5}{2}}}\sum_{n=-\infty}^{\infty} e^{-\frac{\pi^2 n^2}{\alpha}}\left(-2\pi^2 n^2 + \alpha\right) = \frac{\sqrt{\pi}}{2\alpha^{\frac{3}{2}}}\left(1 - \left(4\frac{\pi^2}{\alpha} - 2\right)e^{-\frac{\pi^2}{\alpha}} + \mathcal{O}\left(\frac{e^{-\frac{4\pi^2}{\alpha}}}{\alpha}\right)\right) \;,$$

from which one gets

$$R_1(\alpha) = \frac{1}{2\alpha} - \frac{2\pi^2}{\alpha^2}e^{-\frac{\pi^2}{\alpha}} + \mathcal{O}(e^{-\frac{4\pi^2}{\alpha}}/\alpha) \;. \tag{114}$$

More generally, one can show that, to leading order, $R_k(\alpha)$ is given by

$$R_k(\alpha) \simeq \frac{k}{2\alpha} \;, \tag{115}$$

which indeed satisfies the above Eq. (109). Motivated by the result for $R_1(\alpha)$ (114) we assume that, when $\alpha \to 0$, the leading correction to (115) is of the form

$$R_k(\alpha) = \frac{k}{2\alpha} + c_k(\alpha) e^{-\frac{\pi^2}{\alpha}} + \mathcal{O}(e^{-\frac{4\pi^2}{\alpha}}/\alpha) \,, \tag{116}$$

such that $c_k(\alpha) e^{-\frac{\pi^2}{\alpha}} \ll 1$. Note that from (108) and (114) one has

$$c_0(\alpha) = 0 \,, \; c_1(\alpha) = -2\frac{\pi^2}{\alpha^2} \,. \tag{117}$$

By inserting this ansatz (116) into the above recursion relation satisfied by $R_k(\alpha)$ (109), assuming that $c_k(\alpha) e^{-\frac{\pi^2}{\alpha}} \ll 1$, one finds the following recursion relation for $c_k(\alpha)$:

$$c_{k+1}(\alpha) - c_{k-1}(\alpha) = -\frac{2}{k} c_k(\alpha) - \frac{2\alpha}{k} c_k'(\alpha) - \frac{2\alpha}{k} \frac{\pi^2}{\alpha^2} c_k(\alpha) \,. \tag{118}$$

Following Ref. [30] we introduce the new variable

$$\xi = \frac{\pi^2}{\alpha} \tag{119}$$

and rewrite

$$c_k(\alpha) = -\frac{2}{\pi^2} \xi^2 G_k(\xi) \,, \tag{120}$$

such that $G_k(\xi)$ satisfies the recurrence relation, obtained from (118),

$$G_{k+1}(\xi) - G_{k-1}(\xi) = \frac{2}{k} \left[\xi G_k'(\xi) + G_k(\xi) - \xi G_k(\xi) \right] \,. \tag{121}$$

From Eqs. (117) and (121) one obtains explicit expressions for the first G_k's as

$$G_0(\xi) = 0 \,, \; G_1(\xi) = 1 \,, G_2(\xi) = -2\xi + 2 \,, G_3(\xi) = 2\xi^2 - 6\xi + 3 \,. \tag{122}$$

This recursion relation (121) can be solved by introducing the generating function

$$\tilde{G}(\xi, z) = \sum_{k=1}^{\infty} G_k(\xi) \, z^k \,, \tag{123}$$

which satisfies the partial differential equation (pde)

$$(1 - z^2) \frac{\partial \tilde{G}}{\partial z} - 2\xi \frac{\partial \tilde{G}}{\partial \xi} = \left(z + \frac{1}{z} - 2(\xi - 1) \right) \tilde{G} \,, \tag{124}$$

where we have used the short notation $\tilde{G} \equiv \tilde{G}(\xi, z)$. This pde (124) admits the following exact solution [30]

$$\tilde{G}(\xi, z) = \frac{z}{(1-z)^2} \exp\left(-\frac{2\xi z}{1 - z} \right) \,, \tag{125}$$

from which $G_k(\xi)$ is readily obtained as

$$G_k(\xi) = \oint_{C_z} \frac{dz}{2\pi i} \frac{1}{z^{k+1}} \tilde{G}(\xi, z) = \oint_{C_t} \frac{dt}{2\pi i} e^{-2\xi t} \left(1 + \frac{1}{t} \right)^k \,, \tag{126}$$

where we have performed the change of variable $t = z/(1-z)$. In the above expression the contour C_z encircles the origin $z = 0$ in such a way that $z = 1$ is outside of the contour while the contour C_t encircles the origin $t = 0$ and passes to the right of $t = -1$. One recognizes from Eq. (126), for instance by expanding $(1 + 1/t)^k$ in powers of $1/t$ and integrating term by term that $G_k(\xi)$ can be written as

$$G_k(\xi) = \sum_{m=0}^{k-1} \frac{(-1)^m}{m!} \frac{k!}{(m+1)!(k-m-1)!} (2\xi)^k = L_{k-1}^{(1)}(2\xi) \, , \tag{127}$$

where $L_{k-1}^{(1)}(x)$ are generalized Laguerre polynomials [67]. Therefore one gets, coming back to the variable $\alpha = \frac{\pi^2}{2L^2}$ (119), when $\alpha \to 0$

$$R_k(\alpha) = \frac{k}{2\alpha} - 2\frac{\pi^2}{\alpha^2} L_{k-1}^{(1)}\left(\frac{2\pi^2}{\alpha}\right) e^{-\frac{\pi^2}{\alpha}} + \mathcal{O}(e^{-4\frac{\pi^2}{\alpha}}/\alpha) \, . \tag{128}$$

We now want to analyze this formula for $R_k(\alpha)$ (128) when $k \sim \mathcal{O}(N)$ is large, see Eq. (110). For this purpose, we analyze the integral formula for $G_k(\xi)$ in Eq. (126) using the saddle point method and write

$$G_k(\xi) = \oint_{C_t} \frac{dt}{2\pi i} e^{-2\xi t + k \ln(1+1/t)} \, , \tag{129}$$

which we analyze in the limit where $k, \xi \gg 1$ and $N \gg 1$ such that

$$\frac{k}{N} = y \, , \; \frac{\xi}{N} = \frac{2L^2}{N} = T \, , \tag{130}$$

with y and T kept fixed. Therefore from Eq. (129) one has

$$G_k(\xi) = \oint_{C_t} \frac{dt}{2\pi i} e^{-NS(t)} \, , \; S(t) = 2T\, t - y \ln\left(1 + \frac{1}{t}\right) \, , \tag{131}$$

which can then be evaluated by a saddle point method when $N \to \infty$. This saddle point is such that $dS/dt|_{t=t^*} = 0$, where $S(t)$ reaches its maximum on the real axis, yielding

$$t^* = \frac{-1 + \sqrt{1 - 2y/T}}{2} \, . \tag{132}$$

It corresponds indeed to a maximum of $S(t)$ on the real line

$$S''(t^*) = -y \frac{2t^* + 1}{(t^*(1+t^*))^2} < 0 \, . \tag{133}$$

Note that this saddle point solution (132) makes sense if and only if t^* is real, which implies

$$2\frac{y}{T} < 1 \Rightarrow k < \frac{\xi}{2} = L^2 \, . \tag{134}$$

Now given that the largest value of k involved in the expression of $\tilde{F}_L(N)$ in Eq. (110) is $k = 2N + 1$, this means that this saddle point analysis holds for

$$L > \sqrt{2N} \, , \tag{135}$$

which thus allows to study the right tail of the distribution. This yields finally

$$G_k(\xi) \simeq -\frac{1}{\sqrt{2\pi}} \frac{e^{-NS(t^*)}}{\sqrt{N|S''(t^*)|}} , \tag{136}$$

where the minus sign in Eq. (136) comes from the fact that the integral over the contour C_t in Eq. (129) is counterclockwise oriented, which thus runs, close to t^* from $\Im(t) > 0$ to $\Im(t) < 0$ and hence the minus sign. One finally obtains, plugging the explicit expression of t^* (132) into Eq. (136)

$$G_k(\xi) e^{-\xi} \simeq \frac{(-1)^{k-1}}{4} \frac{1}{\sqrt{\pi \xi}} \sqrt{\frac{2k}{\xi}} \left(1 - \frac{2k}{\xi}\right)^{-\frac{1}{4}} \exp\left(-\xi \gamma\left(\frac{2k}{\xi}\right)\right) , \tag{137}$$

$$\gamma(x) = \sqrt{1-x} - \frac{x}{2} \ln\left(\frac{1+\sqrt{1-x}}{1-\sqrt{1-x}}\right) , \tag{138}$$

where the prefactor $(-1)^k$ in Eq. (137) comes the fact that $1 + 1/t^* < 0$ such that when one evaluates $e^{-NS(t^*)}$ there is a $(-1)^k$ prefactor coming from $\exp[k \ln(1 + 1/t^*)]$ (131). Note in particular the asymptotic behavior of $\gamma(x)$

$$\gamma(x) \sim \frac{2}{3}(1-x)^{\frac{3}{2}} , \; x \to 1 , \tag{139}$$

which will be useful in the following to understand the matching between large and typical fluctuations. Finally one has in this regime (130):

$$R_k(\alpha) = \frac{k}{2\pi^2}\xi + (-1)^k \frac{\xi\sqrt{k}}{2^{1/2}\pi^{5/2}} \left(1 - \frac{2k}{\xi}\right)^{-1/4} \exp\left[-\xi\gamma\left(\frac{2k}{\xi}\right)\right] , \tag{140}$$

where we recall that $\xi = \pi^2/\alpha = 2L^2$. We now want to use this asymptotic behavior (140) to study the right tail of the cumulative distribution $\tilde{F}_N(L)$. For this purpose, we start from the expression given in Eq. (97) to write (see Appendix A1)

$$\tilde{F}_N(L) = \frac{\Gamma(N+1)}{\prod_{j=0}^{N-1} \Gamma(2+j)\Gamma(\frac{3}{2}+j)} \alpha^{N^2+\frac{N}{2}} \left[h_0(\alpha) R_1(\alpha)\right]^N \prod_{k=1}^{N-1} \left[R_{2k}(\alpha) R_{2k+1}(\alpha)\right]^{N-k} , \tag{141}$$

with $R_k(\alpha)$ given in Eq. (116), which for $k \sim \mathcal{O}(N)$ reduces to Eq. (140). To study this expression (141) in the large deviation regime, we write $R_k(\alpha)$ as in Eq. (116) and treat the term $c_k(\alpha) e^{-\frac{\pi^2}{\alpha}}$ in perturbation theory. After cumbersome manipulations left in Appendix A we arrive at the following formula

$$\ln \tilde{F}_N(L) = e^{-\xi} \left[G_{2N}(\xi) + I_{2N}(\xi)\right] + \mathcal{O}\left(\exp\left[-2\xi\gamma\left(\frac{2N}{\xi}\right)\right]\right) , \tag{142}$$

in terms of the variable ξ given in Eq. (119) and the functions $G_{2N}(\xi)$ given in Eq. (127) and $I_{2N}(\xi)$ given by

$$I_{2N}(\xi) = -2\xi \sum_{k=0}^{N-1} \frac{G_{2k+1}(\xi)}{2k+1} . \tag{143}$$

This formula in Eq. (142) yields back the formula obtained in Ref. [31] [see their Eq. (28)]. Using the integral representation for $G_k(\xi)$ obtained before in Eq. (126) one can obtain an integral representation for $I_{2N}(\xi)$, see Appendix A, under the form

$$I_{2N}(\xi) = \oint_{C_t} \frac{dt}{2\pi i} \frac{e^{-2\xi t}}{1+2t} \left(1+\frac{1}{t}\right)^{2N} . \tag{144}$$

The analysis of $I_{2N}(\xi)$ in the large deviation regime (130) can then be carried out as before for $G_{2N}(\xi)$. By comparing the two formulas (126) and (144) it is easy to see that in the large L and large N limit one has

$$I_{2N}(\xi) \sim \frac{1}{1+2t^*} G_{2N}(\xi) = \frac{1}{\sqrt{1-4/T}} G_{2N}(\xi) , \tag{145}$$

where we have used the expression for the saddle point in Eq. (132). Finally one obtains that in the large deviation regime

$$\ln \tilde{F}_N(L) \sim - \left[1+\frac{1}{\sqrt{1-4N/\xi}}\right] \frac{1}{2\sqrt{\pi}} \frac{\sqrt{N}}{\xi} \left(1-\frac{4N}{\xi}\right)^{-1/4} \exp\left[-\xi\gamma\left(\frac{4N}{\xi}\right)\right] , \tag{146}$$

which is negative, as it should, since $\tilde{F}_N(L) < 1$. Recalling that $\xi = 2L^2$ one obtains from Eq. (146) the right tail behavior announced above in Eq. (12),

$$\begin{aligned} &1-\tilde{F}_N(L) \simeq \exp\left[-N\phi_A^+(L/\sqrt{2N})\right] , \\ &\phi_A^+(x) = 4x^2\gamma(1/x^2) = 4x\sqrt{x^2-1} - 2\ln\left[2x\left(\sqrt{x^2-1}+x\right)-1\right] , \end{aligned} \tag{147}$$

where we have used the explicit expression of $\gamma(x)$ in Eq. (137). From the asymptotic behavior (139) one gets immediately

$$\phi_A^+(x) = \frac{2^{9/2}}{3}(x-1)^{3/2} + \mathcal{O}\left((x-1)^{5/2}\right) , \; x \to 1^+ , \tag{148}$$

which yields the asymptotic behavior announced above in Eq. (13). Note in particular that if we set L close to $\sqrt{2N}$ such that

$$L = \sqrt{2N} + cN^{-\frac{1}{6}}s , \; c = 2^{-11/6} , \tag{149}$$

one has, using this asymptotic behavior in Eq. (139)

$$\ln \tilde{F}_N(L) \sim -\frac{1}{4\sqrt{\pi}s^{3/4}} e^{-\frac{2}{3}s^{3/2}} - N^{-1/3} \frac{1}{2^{8/3}\sqrt{\pi}s^{1/4}} e^{-\frac{2}{3}s^{3/2}} + \mathcal{O}(N^{-2/3}) , \tag{150}$$

which is useful to study the matching, discussed in section 2, between the right tail and the central part of the distribution, which describes the typical fluctuations around $L = \sqrt{2N}$.

4.4 Double scaling regime

We now focus on the typical fluctuations of the top path and study $\tilde{F}_N(L)$ for L close to $\sqrt{2N}$. This corresponds to a double scaling limit where both L and N are large but such that $L-\sqrt{2N} = \mathcal{O}(N^{-1/6})$. Hence we set

$$L = \sqrt{2N} + cN^{-1/6}s \ , \ c = 2^{-11/6} \ . \tag{151}$$

We define a "running variable" x_k as

$$x_k = n_{cr}^{2/3}\left(1 - \frac{k}{n_{cr}}\right) \ , \ n_{cr} = \frac{\xi}{2} = L^2 \ . \tag{152}$$

The goal is to analyze the recursion relations for $R_k(\alpha)$ in Eq. (109) when k is also of order $\mathcal{O}(N)$. This can be analyzed in this double scaling limit by assuming the following ansatz [30] (which was later on proved rigorously in Ref. [46])

$$\begin{aligned} R_k(\alpha) &= \frac{n_{cr}^2}{\pi^2} + n_{cr}^{5/3} f_1^+(x_k) + n_{cr}^{4/3} f_2^+(x_k) + n_{cr} f_3^+(x_k) + \mathcal{O}(n_{cr}^{2/3}) \ , \ k \text{ even} \ , \\ R_k(\alpha) &= \frac{n_{cr}^2}{\pi^2} + n_{cr}^{5/3} f_1^-(x_k) + n_{cr}^{4/3} f_2^-(x_k) + n_{cr} f_3^-(x_k) + \mathcal{O}(n_{cr}^{2/3}) \ , \ k \text{ odd} \ . \end{aligned} \tag{153}$$

The fact that we assume different functions $f_1^{\pm}, f_2^{\pm}, f_3^{\pm}$ depending on the parity of k is guided by the previous result (140) where we showed that the leading correction comes with an amplitude proportional to $(-1)^k$, hence depending on the parity of k. By substituting this ansatz (153) into the recursion relation in Eq. (109) one obtains that

$$f_1^+(x) = -f_1^-(x) = -f_1(x) \ , \tag{154}$$

where the function f_1 satisfies a Painlevé II equation (PII)

$$f_1''(x) = 4x f_1(x) + \frac{\pi^4}{2} f_1^3(x) \ , \ f_1(x) \underset{x\to\infty}{\sim} -\frac{2^{5/3}}{\pi^2}\mathrm{Ai}(2^{2/3}x) \ , \tag{155}$$

where $\mathrm{Ai}(x)$ is the standard Airy function. Note the minus sign in the asymptotic behavior which is missing in Ref. [30]. It can be expressed in terms of the Hastings-McLeod solution of PII $q(s)$ in Eq. (2) as

$$f_1(x) = -\frac{2^{5/3}}{\pi^2} q(2^{2/3}x) \ , \tag{156}$$

where

$$q''(s) = 2q^3(s) + sq(s) \ , \ q(s) \underset{s\to\infty}{\sim} \mathrm{Ai}(s) \underset{s\to\infty}{\sim} \frac{1}{2\sqrt{\pi}s^{1/4}} e^{-\frac{2}{3}s^{3/2}} \ . \tag{157}$$

One can further show [30] that the functions f_2^+, f_2^- in Eq. (153) satisfy

$$f_2^+(x) + f_2^-(x) = -\frac{2}{\pi^2}x + \frac{\pi^2}{2} f_1^2(x) \ , \tag{158}$$

and that the functions f_3^+, f_3^- in Eq. (153) satisfy

$$f_3^+(x) + f_3^-(x) = \frac{1}{3}x f_1(x) + \pi^2 f_1(x) f_2^-(x) - \frac{\pi^4}{3} f_1^3(x) + \frac{1}{6} f_1''(x) \ . \tag{159}$$

Using this ansatz (153), one can then analyze $\tilde{F}_N(L)$ in the double scaling limit. For this purpose, it is useful to start from Eq. (110): taking the logarithm on both sides and performing the large n_{cr} expansion of the right hand side, one obtains after a tedious though straightforward calculation, using (154, 158):

$$\ln \tilde{F}(L,N+1) + \ln \tilde{F}_{N-1}(L) - 2\ln \tilde{F}_N(L) = -n_{cr}^{-2/3}\frac{\pi^4}{2}\left(f_1^2(x_{2N}) + \frac{2}{\pi^2}f_1'(x_{2N})\right) + n_{cr}^{-1}\frac{\pi^4}{2}\left(f_1(x_{2N})f_1'(x_{2N}) + \frac{1}{\pi^2}f_1''(x_{2N})\right) + \mathcal{O}(n_{cr}^{-4/3}) \; . \tag{160}$$

On the other hand, if we assume the following ansatz for $\ln \tilde{F}_N(L)$

$$\ln \tilde{F}_N(L) = Y(x_{2N}) + n_{cr}^{-1/3}H(x_{2N}) + \mathcal{O}(n_{cr}^{-2/3}) \; , \tag{161}$$

the expansion of the left hand side of Eq. (160) yields

$$\ln \tilde{F}_{N+1}(L) + \ln \tilde{F}_{N-1}(L) - 2\ln \tilde{F}_N(L) = 4n_{cr}^{-2/3}Y''(x_{2N}) + 4n_{cr}^{-1}H''(x_{2N}) + \mathcal{O}(n_{cr}^{-4/3}) \; . \tag{162}$$

Therefore identifying the terms with the same power of n_{cr} in Eqs. (160) and (162) one obtains

$$\begin{aligned} 4Y''(x) &= -\frac{\pi^4}{2}\left(f_1(x)^2 + \frac{2}{\pi^2}f_1'(x)\right) \\ 4H''(x) &= \frac{\pi^4}{2}\left(f_1(x)f_1'(x) + \frac{1}{\pi^2}f_1''(x)\right) \; . \end{aligned} \tag{163}$$

In terms of the variable s defined in Eq. (151) one has from (152)

$$x_{2N} = 2^{-2/3}s \; , \tag{164}$$

and if we define

$$Y(x) = \tilde{Y}(2^{2/3}x) \; , \; H(x) = \tilde{H}(2^{2/3}x) \; , \tag{165}$$

the above equations (163) can then be written in terms of $q(s)$, the Hastings-McLeod solution of PII (2) as

$$\begin{aligned} \tilde{Y}''(s) &= -\frac{1}{2}\left(q^2(s) - q'(s)\right) \\ \tilde{H}''(s) &= 2^{-1/3}\left(q(s)q'(s) - \frac{1}{2}q''(s)\right) = -2^{-1/3}Y'''(s) \; . \end{aligned} \tag{166}$$

Therefore, from Eqs (161), (165) together with Eq. (166) one obtains, using that $\tilde{F}_N(L \to \infty) = 1$

$$\ln \tilde{F}_N(\sqrt{2N} + 2^{-11/6}N^{-1/6}s) = \tilde{Y}(s) - N^{-1/3}2^{-2/3}\tilde{Y}'(s) + \mathcal{O}(N^{-2/3}) \tag{167}$$

$$Y(s) = -\frac{1}{2}\int_s^\infty (x-s)q^2(x)\,dx - \frac{1}{2}\int_s^\infty q(x)\,dx \; . \tag{168}$$

So that finally one has

$$\tilde{F}_N(\sqrt{2N} + 2^{-11/6}N^{-1/6}s) = \mathcal{F}_1(s) - N^{-1/3}2^{-2/3}\mathcal{F}_1'(s) + \mathcal{O}(N^{-2/3}) \; . \tag{169}$$

Note that using the large s behavior of $q(s)$ in Eq. (157) one obtains the large s behavior of $\mathcal{F}_1(s)$ as:

$$\ln \mathcal{F}_1(s) \sim -\frac{1}{2}\int_s^\infty q(x)\,dx \sim -\frac{1}{4\sqrt{\pi}s^{3/4}}e^{-\frac{2}{3}s^{3/2}}(1 + \mathcal{O}(s^{-3/2})) \; , \tag{170}$$

and therefore, expanding each term of the large N expansion in Eq. (169) for large s, one gets

$$\ln \tilde{F}_N(\sqrt{2N} + 2^{-11/6} N^{-1/6} s) = -\frac{1}{4\sqrt{\pi} s^{3/4}} e^{-\frac{2}{3}s^{3/2}} (1 + \mathcal{O}(s^{-3/2})) \\ - N^{-1/3} \frac{1}{2^{8/3}\sqrt{\pi} s^{1/4}} e^{-\frac{2}{3}s^{3/2}} (1 + \mathcal{O}(s^{-3/2})) + \mathcal{O}(N^{-2/3}) \,. \tag{171}$$

This expansion matches perfectly with the large deviation behavior obtained above in Eq. (150). We notice that this is not only true for the leading term of order $\mathcal{O}(N^0)$ but also for the subleading one, of order $\mathcal{O}(N^{-1/3})$.

Although the leading term in Eq. (169) was already obtained in Ref. [19], and subsequently shown rigorously in [46], we also obtain here the first correction, of order $\mathcal{O}(N^{-1/3})$ to $\mathcal{F}_1$. Note that this correction, being proportional to $\mathcal{F}_1'(s)$, can also be written as a simple shift of the argument of $\mathcal{F}_1$ as

$$\tilde{F}_N(\sqrt{2N} + 2^{-11/6} N^{-1/6} s) = \mathcal{F}_1(s - N^{-1/3} 2^{-2/3}) + \mathcal{O}(N^{-2/3}) \,, \tag{172}$$

such that this leading correction only affects the first moment, the finite N corrections to the higher cumulants being at least of order $\mathcal{O}(N^{-2/3})$ (see also Ref. [68] for a related computation in a sightly different context).

5 Large N analysis of the reunion probability of N non-intersecting Brownian motions on a circle

In this section we focus on the ratio between reunion probabilities $\tilde{G}_N(L)$ for non-intersecting Brownian motions on a circle, i.e. with periodic boundary conditions. We start with the expression given in section 2 in Eq. (19)

$$\tilde{G}_N(L) = \frac{B_N}{L^{N^2}} \sum_{n_1=-\infty}^{\infty} \cdots \sum_{n_N=-\infty}^{\infty} \Delta_N^2(n_1, \cdots, n_N)\, e^{-\frac{2\pi^2}{L^2}\sum_{j=1}^N n_j^2} \tag{173}$$

where $\Delta_N(y_1, \cdots, y_N)$ is the Vandermonde determinant (58) and the prefactor B_N is given by

$$B_N = \frac{1}{(2\pi)^{N/2-N^2} \prod_{j=0}^{N-1} \Gamma(j+2)} \,. \tag{174}$$

Here we introduce the parameter α defined as

$$\alpha = \frac{2\pi^2}{L^2} \,, \tag{175}$$

and rewrite

$$\tilde{G}_N(L) = \frac{\alpha^{N^2/2}}{\prod_{j=0}^{N-1} \Gamma(j+2) 2^{N/2(1-N)} \pi^{N/2}} \sum_{n_1=-\infty}^{\infty} \cdots \sum_{n_N=-\infty}^{\infty} \Delta_N(n_1, \cdots, n_N)^2 e^{-\alpha \sum_{j=1}^N n_j^2} \,. \tag{176}$$

Note that, for simplicity, we use the same notation α as in model A, and in model C below, although its relation to L differs from one model (60), (199) to another (175).

5.1 Coulomb gas analysis for large N and the left tail of $\tilde{G}_N(L)$

This case corresponds exactly, up to a multiplicative prefactor, to the partition function of Yang-Mills theory on the sphere with the gauge group U(N), which was analyzed by Douglas and Kazakov in Ref. [29]. The transposition of their results to the present study was already presented in Ref. [19]. There it was shown that the transition for $\tilde{G}_N(L)$ happens for $L = 2\sqrt{N}$ such that, if one introduces the parameter $r = L/2\sqrt{N}$ one has, similarly to what we have obtained before for model A (88)

$$\lim_{N\to\infty} -\frac{1}{N^2}\ln G_N(\sqrt{4N}\, r) = \begin{cases} 0\ ,\ r \geq 1 \\ \phi_B^-(r) = \frac{1}{2}\phi_A^-(r)\ ,\ r < 1\ , \end{cases} \tag{177}$$

where the function ϕ_A^- is defined in Eq. (88). Here, the asymptotic behavior of $\tilde{G}_N(2\sqrt{N}\, r)$ for r close to 1 is thus

$$\tilde{G}_N(\sqrt{4N}r) \sim \exp\left(-\frac{8}{3}N^2(1-r)^3\right)\ . \tag{178}$$

These results in Eq. (177) and Eq. (178) yield the behaviors announced in section 2 in Eqs (22), (23), for the left tail of $\tilde{G}_N(L)$. However, as before for model A, this saddle point method does not give anything meaningful for the right tail, which can be analyzed using the method of discrete orthogonal polynomials described before.

5.2 Analysis of the right tail of $\tilde{G}_N(L)$

The right hand side of Eq. (176) can be conveniently expressed in terms of the orthogonal polynomials $p_k(n)$ introduced and studied above (93) where α is now defined by (175). Using standard manipulations (in particular the Cauchy-Binet formula), one arrives at

$$\tilde{G}_N(L) = \frac{\alpha^{N^2/2}\Gamma(N+1)}{\prod_{j=0}^{N-1}\Gamma(j+2)2^{N/2(1-N)}\pi^{N/2}}\prod_{j=0}^{N-1} h_j(\alpha)\ . \tag{179}$$

As we have done before (141), this product of the amplitudes h_j in Eq. (179) can be re-written in terms of the R_k's. Substituting then the expression for R_k's in Eq. (103) and treating the terms $c_k(\alpha)e^{-\frac{\pi^2}{\alpha}}$ in perturbation theory, one obtains (see also Ref. [30])

$$\ln\tilde{G}_N(L) = 2e^{-\xi}G_N(\xi) + \mathcal{O}\left(\exp\left[-2\xi\gamma\left(\frac{2N}{\xi}\right)\right]\right)\ , \tag{180}$$

in terms of the variable $\xi = \pi^2/\alpha = L^2/2$, reminding that $\alpha = 2\pi^2/L^2$ in this case (175). This yields, using the expression for $G_N(\xi)$ given in Eq. (137):

$$\ln\tilde{G}_N(L) = \frac{(-1)^{N-1}}{2}\frac{1}{\sqrt{\pi\xi}}\sqrt{\frac{2N}{\xi}}\left(1-\frac{2N}{\xi}\right)^{-1/4}\exp\left[-\xi\gamma\left(\frac{2N}{\xi}\right)\right] \tag{181}$$

$$= \frac{(-1)^{N-1}}{\sqrt{2\pi}L}\sqrt{\frac{4N}{L^2}}\left(1-\frac{4N}{L^2}\right)^{-1/4}\exp\left[-\frac{L^2}{2}\gamma\left(\frac{4N}{L^2}\right)\right]\ , \tag{182}$$

which shows an interesting oscillatory behavior with N: this fact is not problematic as $\tilde{G}_N(L)$ does not have the meaning of a cumulative distribution. One thus obtains from Eq. (181):

$$1-\tilde{G}_N(L) = (-1)^N\exp\left[-N\phi_B^+(L/\sqrt{4N})\right]\ ,\ \phi_B^+(x) = 2x^2\gamma\left(\frac{1}{x^2}\right) = \frac{1}{2}\phi_A^+(x)\ , \tag{183}$$

as announced earlier in section 2 (22), where we have used the expression of $\phi_A^+(x)$ given in Eq. (147). The asymptotic behavior of $\phi_B^+(x)$ when $x \to 1$ follows immediately from Eq. (148), as announced in Eq. (23). Therefore, if we study the regime of L close to $2\sqrt{N}$ and set

$$L = 2\sqrt{N} + 2^{-2/3} N^{-1/6}\, t \;, \tag{184}$$

one obtains from Eq. (181)

$$\ln \tilde{G}_N(L) \sim (-1)^{N-1} N^{-1/3} \frac{1}{2^{4/3}\sqrt{\pi} t^{1/4}} e^{-\frac{2}{3}t^{3/2}} \;, \tag{185}$$

where we notice that this term is of order $\mathcal{O}(N^{-1/3})$: this is responsible for the (mis-)matching with the central part of the distribution, which is instead of order $\mathcal{O}(N^0)$, and described by a double scaling limit which we now focus on.

5.3 Double scaling regime: analysis of the central part of the distribution

To analyze the central part of $\tilde{G}_N(L)$ we start with the following identity, analogous to the one in Eq. (110) for model A, which reads here

$$\frac{\tilde{G}_{N+1}(L)\tilde{G}_{N-1}(L)}{[\tilde{G}_N(L)]^2} = \frac{2\alpha}{N}\frac{h_N}{h_{N-1}} = \frac{2\alpha}{N} R_N(\alpha) \;, \tag{186}$$

which is very useful for asymptotic analysis. Using the asymptotic expansion of $R_N(\alpha)$ in Eq. (153), one can expand the right hand side of Eq. (186) as

$$\ln\left(\frac{2\alpha}{N} R_N(\alpha)\right) = (-1)^{N-1}\pi^2 f_1(x_N) n_{cr}^{-1/3} - \frac{\pi^4}{4} f_1(x_N)^2 n_{cr}^{-2/3} + \mathcal{O}(n_{cr}^{-1}) \;, \tag{187}$$

where n_{cr} is given here by

$$n_{cr} = \frac{L^2}{4} \;. \tag{188}$$

On the other hand, guided by the result which we have obtained for the right tail of $\tilde{G}_N(L)$ and also by the expansion above (187), one assumes the following ansatz for $\ln \tilde{G}_N(L)$ in the double scaling regime

$$\ln \tilde{G}_N(L) = Y(x_N) + (-1)^{N-1} n_{cr}^{-1/3} H(x_N) \;, \tag{189}$$

such that the left hand side of Eq. (186) admits the following expansion

$$\ln \tilde{G}_{N+1}(L) + \ln \tilde{G}_{N-1}(L) - 2\ln \tilde{G}_N(L) = (-1)^N n_{cr}^{-1/3} 4H(x_N) + n_{cr}^{-2/3} Y''(x_N) + \mathcal{O}(n_{cr}^{-1}) \;. \tag{190}$$

Therefore, identifying the different powers of n_{cr} in Eqs. (187) and (190) one finds

$$Y''(x) = -\frac{\pi^4}{4} f_1(x)^2 \;,\; H(x) = -\frac{\pi^2}{4} f_1(x) \;. \tag{191}$$

If we set

$$Y(x) = \tilde{Y}(2^{2/3}x) \;,\; H(x) = \tilde{H}(2^{2/3}x) \;, \tag{192}$$

one has from Eq. (191)

$$\tilde{Y}''(s) = -q^2(s) \;,\; \tilde{H}(s) = 2^{-1/3} q(s) \;. \tag{193}$$

One thus obtains

$$\ln \tilde{G}_N(2\sqrt{N} + 2^{-2/3} s N^{-1/6}) = \tilde{Y}(s) + (-1)^{N-1} N^{-1/3} 2^{-1/3} q(s) + \mathcal{O}(N^{-2/3}) \tag{194}$$

$$\tilde{Y}(s) = -\int_s^\infty (x-s) q^2(x)\, dx \,, \tag{195}$$

which yields

$$\lim_{N\to\infty} \tilde{G}_N(2\sqrt{N} + 2^{-2/3} s N^{-1/6}) = \mathcal{F}_2(s) \,. \tag{196}$$

The result in Eq. (190) yields the formula given in Eq. (27) in section 2. At variance with model A (and model C discussed below) the competition between the two terms $\mathcal{F}_2(s) \sim \exp(-\frac{4}{3}s^{3/2})$ and $q(s) \sim \exp(-\frac{2}{3}s^{3/2})$ yields an unconventional crossover regime discussed in section 2 and illustrated in Fig. 3, which is peculiar to this vicious walker problem.

6 Large N analysis of the reunion probability of N non-intersecting Brownian motions with reflecting boundary conditions

In this section we focus on the ratio of reunion probabilities $\tilde{E}_N(L)$ for non-intersecting Brownian motions on the segment $[0, L]$ with reflecting boundary conditions at $x = 0$ and $x = L$. We start with the expression given in section 2 in Eq. (31)

$$\tilde{E}_N(L) = \frac{C_N}{L^{2N^2-N}} \sum_{n_1=-\infty}^{\infty} \cdots \sum_{n_N=-\infty}^{\infty} \Delta^2(n_1^2, \ldots, n_N^2) e^{-\frac{\pi^2}{2L^2}\sum_{j=1}^N n_j^2} \,, \tag{197}$$

where $\Delta_N(y_1, \cdots, y_N)$ is the Vandermonde determinant (58) and the prefactor C_N given by

$$C_N = \frac{\pi^{2N^2-N}\, 2^{N/2-N^2}}{\prod_{j=0}^{N-1} \Gamma(2+j)\Gamma(1/2+j)} \,, \tag{198}$$

ensures that $\tilde{E}_N(L \to \infty) = 1$. Here we introduce the parameter α given, as in model A (60), by

$$\alpha = \frac{\pi^2}{2L^2} \,, \tag{199}$$

and write

$$\tilde{E}_N(L) = \frac{\alpha^{N^2-\frac{N}{2}}}{\prod_{j=0}^{N-1} \Gamma(2+j)\Gamma(1/2+j)} \sum_{n_1=-\infty}^{\infty} \cdots \sum_{n_N=-\infty}^{\infty} \Delta^2(n_1^2, \ldots, n_N^2) e^{-\alpha \sum_{j=1}^N n_j^2} \,. \tag{200}$$

6.1 Coulomb gas analysis for large N and the left tail of $\tilde{E}_N(L)$

The Coulomb gas analysis of $\tilde{E}_N(L)$, which amounts to the study of the path-integral (over the density $\tilde{\rho}$) entering the expression of $\tilde{E}_N(L)$ as in Eq. (68), is exactly the same as the one done for $\tilde{F}_N(L)$. Indeed the difference between $\tilde{F}_N(L)$ and $\tilde{E}_N(L)$ is the presence, in the expression for $\tilde{F}_N(L)$, of the product $\prod_{i=1}^N n_i^2$. But this term does not contribute to $S[\tilde{\rho}]$ as $\ln \prod_{i=1}^N n_i^2 \sim \mathcal{O}(N)$,

and are thus subdominant compared to $\mathcal{O}(N^2)$ terms which contribute to $S[\tilde{\rho}]$. Therefore one gets immediately the result for the left tail of $\tilde{E}_N(L)$

$$\lim_{N\to\infty} -\frac{1}{N^2}\ln \tilde{E}_N(h\sqrt{2N}) = \begin{cases} 0\ ,\ h \geq 1 \\ \phi_C^-(h) = \phi_A^-(h)\ ,\ h < 1\ , \end{cases} \tag{201}$$

where the rate function $\phi_A^-(h)$ is given in Eq. (88). This yields the result for the left tail of $\tilde{E}_N(L)$ announced in Ref. (34).

6.2 Analysis of the right tail of $\tilde{E}_N(L)$

The expression above (200) can be conveniently expressed in terms of the orthogonal polynomials $p_k(n)$ introduced and studied above (93) where $\alpha = \pi^2/2L^2$ (199). Using the identity

$$\Delta_N(n_1^2, \cdots, n_N^2) = \det_{1\leq i,j\leq N} [p_{2i-2}(n_j)]\ , \tag{202}$$

and the Cauchy-Binet formula, one arrives at

$$\tilde{E}_N(L) = \frac{\alpha^{N^2-\frac{N}{2}}}{\prod_{j=1}^{N-1}\Gamma(2+j)\Gamma(1/2+j)} \prod_{j=1}^{N} h_{2j-2}(\alpha)\ . \tag{203}$$

As we have done before (141), this product of the amplitudes h_j in Eq. (203) can be re-written in terms of the R_k's. Substituting then the expression for R_k's in Eq. (103) and treating the terms $c_k(\alpha)e^{-\frac{\pi^2}{\alpha}}$ in perturbation theory, one obtains [see also Ref. [31]]

$$\ln \tilde{E}_N(L) = e^{-\xi}\left[G_N(\xi) - I_{2N}(\xi)\right] + \mathcal{O}\left(\exp\left[-2\xi\gamma\left(\frac{2N}{\xi}\right)\right]\right)\ , \tag{204}$$

in terms of the variable $\xi = \pi^2/\alpha = 2L^2$, where we have used $\alpha = \pi^2/2L^2$ (199). Note that this expression is very similar to, albeit different from, the expression obtained for $\ln \tilde{F}_N(L)$ in Eq. (142) (the term $I_{2N}(\xi)$ comes here with a minus sign). One thus gets, from the previous analysis (146),

$$\ln \tilde{E}_N(L) \sim -\left[1 - \frac{1}{\sqrt{1-4N/\xi}}\right]\frac{1}{2\sqrt{\pi}}\frac{\sqrt{N}}{\xi}\left(1-\frac{4N}{\xi}\right)^{-1/4}\exp\left[-\xi\gamma\left(\frac{4N}{\xi}\right)\right]\ . \tag{205}$$

Therefore, one obtains from Eq. (205)

$$1 - \tilde{E}_N(L) = -\exp\left[-N\phi_C^+(L/\sqrt{2N})\right]\ ,\ \phi_C^+(x) = 4x^2\gamma\left(\frac{1}{x^2}\right) = \phi_A^+(x)\ , \tag{206}$$

as announced in Eq. (34). The asymptotic behavior of $\phi_C^+(x)$ when $x \to 1$ follows straightforwardly from Eq. (148). Note in particular that if we set L close to $\sqrt{2N}$ such that

$$L = \sqrt{2N} + cN^{-\frac{1}{6}}s\ ,\ c = 2^{-11/6}\ , \tag{207}$$

one has, from Eq. (205), using the asymptotic behavior for $\gamma(x)$ in Eq. (139)

$$\ln \tilde{E}_N(L) \sim \frac{1}{4\sqrt{\pi}s^{3/4}}e^{-\frac{2}{3}s^{3/2}} - N^{-1/3}\frac{1}{2^{8/3}\sqrt{\pi}s^{1/4}}e^{-\frac{2}{3}s^{3/2}} + \mathcal{O}(N^{-2/3})\ , \tag{208}$$

which is useful to study the matching with the typical fluctuations around $L = \sqrt{2N}$.

6.3 Double scaling regime: analysis of the central part of the distribution

To analyze the central part of $\tilde{E}_N(L)$ we start with the following identity, analogous to the one in Eq. (110) for model A, which reads here

$$\frac{\tilde{E}_{N+1}(L)\tilde{E}_{N-1}(L)}{[\tilde{E}_N(L)]^2} = \frac{\alpha^2}{N(N-1/2)}\frac{h_{2N}}{h_{2N-2}} = \frac{\alpha^2}{N(N-1/2)}R_{2N}(\alpha)R_{2N-1}(\alpha) \ , \tag{209}$$

which is very useful for asymptotic analysis. Using the asymptotic expansion of $R_N(\alpha)$ in Eq. (153), one can expand the right hand side of Eq. (209) as

$$\begin{aligned} \ln\left(\frac{\alpha^2}{N(N-1/2)}R_{2N}(\alpha)R_{2N-1}(\alpha)\right) &= -n_{cr}^{-2/3}\frac{\pi^4}{2}\left(f_1^2(x_{2N}) - \frac{2}{\pi^2}f_1'(x_{2N})\right) \\ &+ n_{cr}^{-1}\frac{\pi^4}{2}\left(-f_1(x_{2N})f_1'(x_{2N}) + \frac{1}{\pi^2}f_1''(x_{2N})\right) + \mathcal{O}(n_{cr}^{-4/3}) \ , \end{aligned} \tag{210}$$

where, here

$$n_{cr} = L^2 \ . \tag{211}$$

On the other hand, if we assume the following ansatz for $\ln \tilde{E}_N(L)$

$$\ln \tilde{E}_N(L) = Y(x_{2N}) + n_{cr}^{-1/3}H(x_{2N}) + \mathcal{O}(n_{cr}^{-2/3}) \ , \tag{212}$$

the expansion of the left hand side of Eq. (210) reads

$$\ln \tilde{E}_{N+1}(L) + \ln \tilde{E}_{N-1}(L) - 2\ln \tilde{E}_N(L) = 4n_{cr}^{-2/3}Y''(x_{2N}) + 4n_{cr}^{-1}H''(x_{2N}) + \mathcal{O}(n_{cr}^{-4/3}) \ . \tag{213}$$

Therefore identifying the terms in Eqs. (210) and Eq. (213) with the same power of n_{cr} one obtains

$$\begin{aligned} 4Y''(x) &= -\frac{\pi^4}{2}\left(f_1(x)^2 - \frac{2}{\pi^2}f_1'(x)\right) \\ 4H''(x) &= -\frac{\pi^4}{2}\left(f_1(x)f_1'(x) - \frac{1}{\pi^2}f_1''(x)\right) \ . \end{aligned} \tag{214}$$

In terms of the variable s defined in Eq. (207) one has from (152)

$$x_{2N} = 2^{-2/3}s \ , \tag{215}$$

and if we define

$$Y(x) = \tilde{Y}(2^{2/3}x) \ , H(x) = \tilde{H}(2^{2/3}x) \ , \tag{216}$$

the above equations (214) can then be written in terms of $q(s)$, the Hastings-McLeod solution of PII (2) as

$$\begin{aligned} \tilde{Y}''(s) &= -\frac{1}{2}\left(q^2(s) + q'(s)\right) \\ \tilde{H}''(s) &= 2^{-1/3}\left(q(s)q'(s) + \frac{1}{2}q''(s)\right) = 2^{-1/3}\tilde{Y}'''(s) \ . \end{aligned} \tag{217}$$

Therefore, from Eqs. (212) and (216) together with Eq. (217) one obtains, using that $\tilde{E}_N(L \to \infty) = 1$

$$\ln \tilde{E}_N(\sqrt{2N} + 2^{-11/6} N^{-1/6} s) = \tilde{Y}(s) + N^{-1/3} 2^{-2/3} \tilde{Y}'(s) + \mathcal{O}(N^{-2/3}) \tag{218}$$

$$Y(s) = -\frac{1}{2} \int_s^\infty (x-s) q^2(x)\, dx + \frac{1}{2} \int_s^\infty q(x)\, dx \, . \tag{219}$$

So that finally one has

$$\tilde{E}_N(\sqrt{2N} + 2^{-11/6} N^{-1/6} s) = \frac{\mathcal{F}_2(s)}{\mathcal{F}_1(s)} + N^{-1/3} 2^{-2/3} \frac{d}{ds} \left[\frac{\mathcal{F}_2(s)}{\mathcal{F}_1(s)} \right] + \mathcal{O}(N^{-2/3}) \, , \tag{220}$$

where we have used the expression of $\mathcal{F}_2$ and $\mathcal{F}_1$ in terms of $q(s)$ given respectively in Eq. (1) and (4). As noticed previously for model A (172), the first correction in Eq. (220), proportional to $N^{-1/3}$, can be absorbed by a shift of the argument $s \to s + 2^{-2/3} N^{-1/3}$. An analogous structure is known for the large N expansion at the soft edge of the Laguerre ensemble in random matrix theory (see [64], eq. (7.162)).

7 Conclusion

To conclude, we have performed in this paper a systematic study of three different models of N non-intersecting Brownian motions on a line segment $[0, L]$ with three different types of boundary conditions at $x = 0$ and $x = L$: absorbing (model A), periodic (model B) and reflecting (model C) boundary conditions. In each of these models we have focused on a normalized reunion probability which, in model A, can also be interpreted as the maximal height of N non-intersecting Brownian excursions on the unit time interval. We have presented a self-contained derivation of the formulas for finite N for these reunion probabilities, whose expressions had been given without the details in previous publications in Ref. [12], for model A, and for model B and C in Ref. [19]. An interesting property of these reunion probabilities is that they are, up to a multiplicative prefactor, identical to the partition function of Yang-Mills theory on the sphere with a gauge group G which is selected by the choice of boundary conditions: $\mathrm{Sp}(2N)$ for model A, $\mathrm{U}(N)$ for model B and $\mathrm{SO}(2N)$ for model C. As a consequence of this correspondence, these reunion probabilities exhibit a third-order phase transition, akin to the Douglas-Kazakov transition in YM_2, as the size of the system L crosses a critical value $L_c(N) \propto \sqrt{N}$ between the left tail $L < L_c(N)$ and the right tail $L > L_c(N)$. In the central part, $L \sim L_c(N)$, these reunion probabilities, converge in a proper scaling limit, when $N \to \infty$, to a limiting form which can be expressed in terms of the Tracy-Widom distributions $\mathcal{F}_1$ and $\mathcal{F}_2$: this fact was certainly one of the main results obtained in Ref. [19]. Here, we have provided a detailed and self-contained derivation of these results. The main emphasis of the paper is on the study of the large deviations of these reunion probabilities both in the right and in the left tail, together with a careful analysis of the matching between the different regimes (left tail, central part and right tail). While this matching in model A and model C is very similar to the one found for the distribution of the largest eigenvalue of GUE, one finds that the situation is much more involved in model B. In this case, there is instead a crossover (see Fig. 3) between the central regime, for $L - 2\sqrt{N} \sim \mathcal{O}(N^{-1/6})$ and the right tail, $L > 2\sqrt{N}$, of the reunion probability, this crossover happening at a crossover length scale $L_{\mathrm{cross}} - 2\sqrt{N} \propto N^{-1/6} (\ln N)^{2/3}$, which seems to be a peculiar feature of these vicious walkers problems.

Acknowledgements This research was partially supported by ANR grant 2011-BS04-013-01 WALKMAT and in part by the Indo-French Centre for the Promotion of Advanced Research under Project 4604-3.

A Details about the large deviation regime

In this appendix, we give some details concerning the calculation of $\tilde{F}_N(L)$ in the large deviation regime.

A.1 Derivation of the formula given in Eq. (141)

We first provide a derivation of the formula given in Eq. (141) starting from (61) and (97). Indeed, from the definition of $R_k(\alpha)$ one has

$$h_1(\alpha) = R_1(\alpha)h_0(\alpha)\ ,\ h_2(\alpha) = R_2(\alpha)h_1(\alpha) = h_0(\alpha)R_1(\alpha)R_2(\alpha)\cdots \tag{221}$$

and more generally

$$h_k(\alpha) = h_0(\alpha)R_1(\alpha)R_2(\alpha)\cdots R_k(\alpha)\ . \tag{222}$$

Therefore, $\Omega_N(\alpha)$ in Eq. (96) can be rewritten as

$$\begin{aligned}\Omega(\alpha,N) &= N!\prod_{j=1}^{N} h_{2j-1}(\alpha) = N!\,[h_0(\alpha)R_1(\alpha)][h_0(\alpha)R_1(\alpha)R_2(\alpha)R_3(\alpha)]\\ &\times [h_0(\alpha)R_1(\alpha)R_2(\alpha)R_3(\alpha)R_4(\alpha)R_5(\alpha)]\cdots\\ &= N![h_0(\alpha)R_1(\alpha)]^N[R_2(\alpha)R_3(\alpha)]^{N-1}[R_4(\alpha)R_5(\alpha)]^{N-2}\cdots\\ &= N![h_0(\alpha)R_1(\alpha)]^N\prod_{k=1}^{N-1}[R_{2k}(\alpha)R_{2k+1}(\alpha)]^{N-k}\end{aligned} \tag{223}$$

which is the formula given in Eq. (141).

A.2 Derivation of the formula given in Eq. (142)

In this appendix we give a detailed derivation, starting from the exact expression of $\tilde{F}_N(L)$ in Eq. (61, 62), of the asymptotic estimate for $\ln\tilde{F}_N(L)$, valid in the limit $L \gg \sqrt{2N} \gg 1$:

$$\ln\tilde{F}_N(L) = e^{-\xi}\left[G_{2N}(\xi) + I_{2N}(\xi)\right]\ , \tag{224}$$

in terms of the variable $\xi = \pi^2/\alpha = 2L^2$ and the functions $G_{2N}(\xi)$ given in Eq. (127) and $I_{2N}(\xi)$ given by

$$I_{2N}(\xi) = -2\xi\sum_{k=0}^{N-1}\frac{G_{2k+1}(\xi)}{2k+1}\ . \tag{225}$$

This formula (224) was given in Ref. [31] [see their Eq. (28)] without any detail: that is the purpose of this appendix to fill this gap by providing a detailed derivation of it.

To study the formula for $\tilde{F}_N(L)$ starting from Eq. (61, 62), we first write the product of the gamma functions in the denominator as

$$\prod_{j=0}^{N-1}\Gamma(2+j)\Gamma\left(\frac{3}{2}+j\right) = \prod_{k=1}^{N}k!\,\Gamma\left(\frac{1}{2}+k\right)\ . \tag{226}$$

Note that the product of factorials can be written as

$$\prod_{k=1}^{N}k! = 2^{N-1}3^{N-2}\cdots N = N!\prod_{k=1}^{N-1}k^{N-k}\ . \tag{227}$$

Similarly, the product of $\Gamma(k+1/2)$ in Eq. (226) can be written as

$$\prod_{k=1}^{N} \Gamma\left(k+\frac{1}{2}\right) = \left(\frac{\Gamma(1/2)}{2}\right)^N \prod_{k=1}^{N-1} (k+\frac{1}{2})^{N-k} \,, \tag{228}$$

where we have used

$$\Gamma(k+1/2) = \left(k-\frac{1}{2}\right)\left(k-\frac{3}{2}\right)\cdots\frac{1}{2}\Gamma\left(\frac{1}{2}\right) \,. \tag{229}$$

Finally, using Eqs (227) and (228) we write Eq. (226) as

$$\prod_{j=0}^{N-1} \Gamma(2+j)\Gamma\left(\frac{3}{2}+j\right) = N!\left(\frac{\sqrt{\pi}}{2}\right)^N \prod_{k=1}^{N-1} k^{N-k} \prod_{k=1}^{N-1} (k+\frac{1}{2})^{N-k} \,, \tag{230}$$

where we have used $\Gamma(1/2)=\sqrt{\pi}$.

Using the ansatz for $R_k(\alpha)$ given in Eq. (116) where we consider $c_k(\alpha)e^{-\pi^2/\alpha} \ll 1$, with $\alpha = \pi^2/2L^2$, we write,

$$h_0(\alpha)R_1(\alpha) = \sqrt{\frac{\pi}{\alpha}}\frac{1}{2\alpha}\left(1+2e^{-\frac{\pi^2}{\alpha}}\right)\left(1+2\alpha c_1(\alpha)e^{-\frac{\pi^2}{\alpha}}\right) \tag{231}$$

and for $k \geq 1$

$$R_{2k}(\alpha)R_{2k+1}(\alpha) = \frac{k}{\alpha}\frac{k+1/2}{\alpha}\left[1+\frac{\alpha}{k}c_{2k}(\alpha)e^{-\pi^2/\alpha}\right]\left[1+\frac{\alpha}{k+1/2}c_{2k+1}(\alpha)e^{-\pi^2/\alpha}\right] + \mathcal{O}(e^{-2\pi^2/\alpha}) \tag{232}$$

so that, using the formula in Eq. (230) one obtains that $\tilde{F}_N(L)$ in Eq. (61, 62) can be written as

$$\begin{aligned}\tilde{F}_N(L) = &\left(1+2e^{-\frac{\pi^2}{\alpha}}\right)^N \left(1+2\alpha c_1(\alpha)e^{-\frac{\pi^2}{\alpha}}\right)^N \\ &\times \prod_{k=1}^{N-1}\left(1+\frac{\alpha}{k}c_{2k}(\alpha)e^{-\frac{\pi^2}{\alpha}}\right)^{N-k} \prod_{k=1}^{N-1}\left(1+\frac{\alpha}{k+1/2}c_{2k+1}(\alpha)e^{-\frac{\pi^2}{\alpha}}\right)^{N-k} \,.\end{aligned} \tag{233}$$

We now perform the expansion of this expression (233), considering $c_k(\alpha)e^{-\pi^2/\alpha} \ll 1$. It is more convenient to expand its logarithm $\ln \tilde{F}_N(L)$ which using the explicit expression for $c_1(\alpha)$ in Eq. (117) together with the expression of $c_k(\alpha)$ in terms of $G_k(\xi)$ in Eq. (120), can be written as a function of $\xi = \pi^2/\alpha$ as

$$\begin{aligned}\ln \tilde{F}_N(L) &= -2N(2\xi-1)e^{-\xi} - 2\xi e^{-\xi}\sum_{k=1}^{N-1}\left(\frac{N-k}{k}G_{2k}(\xi) + \frac{N-k}{k+1/2}G_{2k+1}(\xi)\right) \\ &= 2Ne^{-\xi} - 2\xi e^{-\xi}\left(\sum_{k=1}^{N-1}\frac{2N-2k}{2k}G_{2k}(\xi) + \sum_{k=0}^{N-1}\frac{2N-2k}{2k+1}G_{2k+1}(\xi)\right)\end{aligned} \tag{234}$$

where we have used $G_1(\xi)=1$. It is then possible to write these two sums in Eq. (234) as

$$\ln \tilde{F}_N(L) = 2N\, e^{-\xi} - 2\xi e^{-\xi}\left(\sum_{j=1}^{2N-1}\frac{2N-j}{j}G_j(\xi) + \sum_{k=0}^{N-1}\frac{G_{2k+1}(\xi)}{2k+1}\right) \,. \tag{235}$$

Finally, using the following identity satisfied by the polynomials $G_k(\xi)$ [30]

$$2N - 2\xi\sum_{j=1}^{2N-1}\frac{2N-j}{j}G_j(\xi) = G_{2N}(\xi) \,, \tag{236}$$

which can be shown, for instance, by using their explicit expression of $G_k(\xi)$ (127), one obtains finally

$$\ln \tilde{F}_N(L) = e^{-\xi}\left(G_{2N}(\xi) + I_{2N}(\xi)\right) \,, \tag{237}$$

as given in the text in Eq. (142).

A.3 An integral representation for $I_{2N}(\xi)$ in Eq. (143)

We start with the integral representation for $G_k(\xi)$ in Eq. (126) to express $I_{2N}(\xi)$ in Eq. (143) as

$$I_{2N}(\xi) = -2\xi \oint_{C_t} \frac{dt}{2\pi i} e^{-2\xi t} \sum_{k=0}^{N-1} \frac{1}{2k+1} \left(1+\frac{1}{t}\right)^{2k+1} . \tag{238}$$

Performing an integration by part one obtains

$$I_{2N}(\xi) = \oint_{C_t} \frac{dt}{2\pi i} \frac{e^{-2\xi t}}{t^2} \sum_{k=0}^{N-1} \left(1+\frac{1}{t}\right)^{2k} . \tag{239}$$

By performing the sum over k in (239) and dropping an N-independent constant term, one finally arrives at the expression given in the text in Eq. (144).

References

1. P. G. de Gennes, *Soluble model for fibrous structures with steric constraints*, J. Chem. Phys. **48**, 2257-2259 (1968).
2. M. E. Fisher, *Walks, walls, wetting, and melting*, J. Stat. Phys. **34**, 667-728 (1984).
3. C. Krattenthaler, A. J. Guttmann, and X. G. Viennot, *Vicious walkers, friendly walkers and Young tableaux: II. With a wall*, J. Phys. A: Math. Gen. **33**, 8835-8866 (2000).
4. J. Baik, *Random vicious walks and random matrices*, Comm. Pure Appl. Math. **53**, 1385–1410 (2000).
5. P. J. Forrester, *Random walks and random permutations*, J. Phys. A **34**, L417-L423 (2001).
6. K. Johansson, *Discrete Polynuclear Growth and Determinantal Processes*, Commun. Math. Phys. **242**, 277-329 (2003).
7. T. Nagao, *Dynamical correlations for vicious random walk with a wall*, Nucl. Phys. B **658**, 373–396 (2003).
8. M. Katori and H. Tanemura, *Symmetry of matrix-valued stochastic processes and noncolliding diffusion particle systems* J. Math. Phys. **45**, 3058-3086 (2004).
9. P. Ferrari and M. Praehofer, *One-dimensional stochastic growth and Gaussian ensembles of random matrices*, Proc. Inhomogeneous Random Systems 2005, Markov Processes Relat. Fields, **12**, 203-234 (2006).
10. C. A. Tracy and H. Widom, *Non-intersecting Brownian excursions*, Ann. Appl. Probab. **17**, 953-979 (2007).
11. E. Daems and A. B. J. Kuijlaars, *Multiple orthogonal polynomials of mixed type and non-intersecting Brownian motions*, J. Approx. Theor. **146**, 91-114 (2007).
12. G. Schehr, S. N. Majumdar, A. Comtet, and J. Randon-Furling, *Exact distribution of the maximal height of p vicious walkers*, Phys. Rev. Lett. **101**, 150601 (2008).
13. C. Nadal and S. N. Majumdar, *Non-intersecting Brownian Interfaces and Wishart Random Matrices*, Phys. Rev. E **79**, 061117 (2009).
14. J. Novak, *Vicious walkers and random contraction matrices*, Int. Math. Res. Not. **2009**, 3310–3327 (2009).
15. J. Rambeau and G. Schehr, *Extremal statistics of curved growing interfaces in* $1+1$ *dimensions*, Europhys. Lett. **91**, 60006 (2010).
16. A. Borodin and J. Kuan, *Random surface growth with a wall and Plancherel measures for* $O(\infty)$, Commun. Pure Appl. Math. **63**, 831–894 (2010).
17. P. Bleher, S. Delvaux and A. B. J. Kuijlaars, *Random matrix model with external source and a constrained vector equilibrium problem*, Commun. Pure Appl. Math. **64**, 116–160 (2011).
18. M. Adler, P. van Moerbeke and D. Vanderstichelen, *Non-intersecting Brownian motions leaving and going to several points*, Physica D **241**, 443–460 (2012).
19. P. J. Forrester, S. N. Majumdar, G. Schehr, *Non-intersecting Brownian walkers and Yang-Mills theory on the sphere*, Nucl. Phys. B **844**, 500-526 (2011); Erratum Nucl. Phys. B **857**, 424-427 (2011).
20. S. de Haro and M. Tierz, *Brownian motion, Chern-Simons theory, and 2d Yang-Mills*, Phys, Lett. B **201**, 201–208 (2004).
21. C. Nadal, S. N. Majumdar, *A simple derivation of the Tracy-Widom distribution of the maximal eigenvalue of a Gaussian unitary random matrix*, J. Stat. Mech., P04001 (2011).
22. P. Vivo, S. N. Majumdar and O, Bohigas, *Distributions of Conductance and Shot Noise and Associated Phase Transitions*, Phys. Rev. Lett. **101**, 216809 (2008).

23. P. Vivo, S. N. Majumdar and O, Bohigas, *Probability Distributions of Linear Statistics in Chaotic Cavities and Associated Phase Transitions*, Phys. Rev. B **81**, 104202 (2010).
24. K. Damle, S.N. Majumdar, V. Tripathi, and P. Vivo, *Phase Transitions in the Distribution of the Andreev Conductance of Superconductor-Metal Junctions with Many Transverse Modes*, Phys. Rev. Lett., **107**, 177206 (2011).
25. C. Nadal, S. N. Majumdar, and M. Vergassola, *Phase Transitions in the Distribution of Bipartite Entanglement of a Random Pure State*, Phys. Rev. Lett. **104**, 110501 (2010).
26. C. Nadal, S. N. Majumdar, and M. Vergassola, *Statistical Distribution of Quantum Entanglement for a Random Bipartite State*, J. Stat. Phys. **142**, 403–438 (2011).
27. C. A. Tracy and H. Widom, *Level-spacing distributions and the Airy kernel*, Commun. Math. Phys. **159**, 151–174 (1994).
28. C. A. Tracy and H. Widom, *On orthogonal and symplectic matrix ensembles*, Commun. Math. Phys. **177**, 727–754 (1996).
29. M. R. Douglas, V. A. Kazakov, *Large N phase transition in continuum QCD_2*, Phys. Lett. B **319**, 219-230 (1993).
30. D. J. Gross, A. Matytsin, *Instanton Induced Large N Phase Transitions in Two and Four Dimensional QCD*, Nucl. Phys. B. **429**, 50-74 (1994).
31. M. Crescimanno, S. G. Naculich, H. J. Schnitzer, *Evaluation of the free energy of two-dimensional Yang-Mills theory*, Phys. Rev. D **54**, 1809-1813 (1996).
32. D.S. Dean, S. N. Majumdar, *Large deviations of extreme eigenvalues of random matrices*, Phys. Rev. Lett. **97**, 160201 (2006).
33. P. Vivo, S. N. Majumdar, O. Bohigas, *Large deviations of the maximum eigenvalue in Wishart random matrices*, J. Phys. A: Math. Theor. **40**, 4317-4337 (2007).
34. D. S. Dean and S. N. Majumdar, *Extreme value statistics of eigenvalues of Gaussian random matrices*, Phys. Rev. E **77**, 041108 (2008).
35. S.N. Majumdar and M. Vergassola, *Large deviations of the maximum eigenvalue for Wishart and Gaussian random matrices*, Phys. Rev. Lett. **102**, 060601 (2009).
36. G. Borot, B. Eynard, S. N. Majumdar and C. Nadal, *Large deviations of the maximal eigenvalue of random matrices*, J. Stat. Mech., P11024 (2011).
37. P. J. Forrester, *Spectral density asymptotics for Gaussian and Laguerre β-ensembles in the exponentially small region*, J. Phys. A **45**, 075206 (2012).
38. N. Bonichon and M. Mosbah, *Watermelon uniform random generation with applications*, Theor. Comput. Sci. **307**, 241–256 (2003).
39. D. J. Grabiner, *Brownian motion in a Weyl chamber, non-colliding particles, and random matrices*, Ann. I.H.P. (B), Prob. Stat. **35**, 177–204 (1999).
40. D. J. Grabiner, *Random Walk in an Alcove of an Affine Weyl Group, and Non-Colliding Random Walks on an Interval*, J. Combin. Theory Ser. A **97**, 285–306 (2002).
41. M. Fulmek, *Asymptotics of the average height of 2 watermelons with a wall*, The Electronic J. Combinatorics **14**(1), R64/1–20 (2007).
42. M. Katori, M. Izumi, Kobayashi, *Two Bessel bridges conditioned never to collide, double Dirichlet series, and Jacobi theta function* , J. Stat. Phys. **131**, 1067–1083 (2008).
43. N. Kobayashi, M. Izumi, M. Katori, *Maximum distributions of bridges of noncolliding Brownian paths*, Phys. Rev. E **78**, 051102 (2008).
44. T. Feierl, *The height of watermelons with wall*, J. Phys. A: Math. Theor. **45**, 095003 (2012).
45. J. Rambeau, G. Schehr, *Distribution of the time at which N vicious walkers reach their maximal height*, Phys. Rev. E **83**, 061146 (2011).
46. K. Liechty, *Non-intersecting Brownian motions on the half-line and discrete Gaussian orthogonal polynomials*, J. Stat. Phys. **147**, 582–622 (2012).
47. A. Borodin, P. L. Ferrari, M. Praehofer, T. Sasamoto and J. Warren, *Maximum of Dyson Brownian motion and non-colliding systems with a boundary*, Electron. Comm. Probab. **14**, 486–494 (2009).
48. M. Prähofer and H. Spohn, *Universal distributions for growth processes in $1+1$ dimensions and random matrices*, Phys. Rev. Lett. **84**, 4882–4885 (1999).
49. M. Prähofer and H. Spohn, *Exact scaling functions for one-dimensional stationary KPZ growth*, J. Stat. Phys. **115** (1-2), 255-279 (2004).
50. G. R. Moreno Flores, J. Quastel, D. Remenik, *Endpoint distribution of directed polymers in 1+1 dimensions*, preprint arXiv:1106.2716, to appear in Commun. Math. Phys.
51. G. Schehr, *Extremes of N vicious walkers for large N: application to the directed polymer and KPZ interfaces*, arXiv:1203.1658.
52. J. Quastel, D. Remenik, *Tails of the endpoint distribution of directed polymers*, arXiv:1203.2907.
53. J. Baik, K. Liechty, G. Schehr, *On the joint distribution of the maximum and its position of the Airy2 process minus a parabola*, arXiv:1205.3665.
54. K. Takeuchi, M. Sano, *Evidence for geometry-dependent universal fluctuations of the Kardar-Parisi-Zhang interfaces in liquid-crystal turbulence*, J. Stat. Phys. **147**, 853–890 (2012).
55. S. Karlin, J. McGregor, *Coincidence probabilities*, Pacific J. Math. **9**, 1141 (1959).

56. B. Lindström, *On the vector representations of induced matroids*, Bull. London Math. Soc., **5**, 85 (1973).
57. I. Gessel, G. Viennot, *Determinants, paths, and plane partitions*, Adv. Math. **58**, 300 (1985).
58. D. J. Gross, E. Witten, *Possible third-order phase transition in the large-n lattice gauge limit*, Physical Review D **21**, 446–453 (1980).
59. S. R. Wadia, $N = \infty$ *phase transition in a class of exactly soluble model lattice gauge theories*, Phys. Lett. **93B**, 403–410 (1980).
60. V. Periwal and D. Shevitz, *Unitary-matrix models as exactly solvable string theories*, Phys. Rev. Lett. **64**, 1326–1329 (1990).
61. F. J. Dyson, *Statistical theory of the energy levels of complex systems. I*, J. Math. Phys. **3**, 140–156 (1962).
62. F. J. Dyson, *Statistical theory of the energy levels of complex systems. II*, J. Math. Phys. **3**, 157-165 (1962).
63. F. J. Dyson, *Statistical theory of the energy levels of complex systems. III*, J. Math. Phys. **3**, 166-174 (1962).
64. P. J. Forrester, *Log-gases and random matrices*, Princeton University Press, Princeton, NJ, 2010.
65. D. J. Gross, A. Matytsin, *Some Properties of Large N Two Dimensional Yang–Mills Theory*, Nucl. Phys. B. **437**, 541 (1995).
66. A. Erdélyi *et al.*, *Higher transcendental functions*, McGraw-Hill (1953).
67. G. Szegö, *Orthogonal polynomials*, American Mathematical Society, Providence R.I., 4th edition, (1975).
68. J. Baik, R. Jenkins, *Limiting distribution of maximal crossing and nesting of Poissonized random matchings*, preprint arXiv:1111.0269, to appear in Ann. Probab.